from Nexus Thinking to Nexus Doing

REXUS

MANAGING RESILIENT NEXUS SYSTEMS THROUGH PARTICIPATORY SYSTEMS DYNAMICS MODELLING

Deliverable 3.9 – Fit-for-Nexus climate projections.

WP3 – REXUS Observatory

www.rexusproject.eu

Edited by: Antoniadou Marina, Christina Papadaskalopoulou, George Kefalas (DRAXIS)

This project has received funding from the European Union's Horizon 2020 research and innovation programme under grant agreement No 101003632.

Document Information

Grant agreement	101003632	**Acronym**	REXUS
Full Title of the Project	Managing REsilient neXUS systems through participatory systems dynamics modelling		
Horizon 2020 call	H2020-LC-CLA-2018-2019-2020 / H2020-LC-CLA-2020-2		
Start Date	1 May 2021	**Duration**	36 months
Project website	www.rexusproject.eu		
Document URL	https://rexusproject.squarespace.com/		
REA Project Officer	Giulio Pattanaro		
Project Coordinator	José González Piqueras		
Deliverable	D3.9- Fit-for-Nexus climate projections		
Work Package	WP3- REXUS Observatory		
Date of delivery	31 December 2021	**Actual**	31 December 2021
Nature	R-Report	**Dissemination Level**	PU
Lead Beneficiary	DRAXIS		
Lead Author	Marina Antoniadou	**Email**	mantoniadou@draxis.gr
Contributors	Christina Papadaskalopoulou, George Kefalas		
Internal Reviewer	UCLM (David Cifuentes, Jesús Garrido and José González)		
Distribution to	All partners		
keywords	Climate projections, climate change, RCP4.5, RCP8.5, reference period, CORDEX, temperature, precipitation, evapotranspiration, ensemble, spread, map, ESGF		

Contents

List of Abbreviations

Abbreviation	Definition
Af	Tropical rainforest climate
C3S	Copernicus Climate Change Service
CORDEX	Coordinated Regional Climate Downscaling Experiment
ESGF	Earth System Grid Federation
GCM	Global Climate Models
GHG	Green House Gases
km	Kilometres
m	Meters
mm	Millimetres
ET	Potential Evapotranspiration
Prec	Precipitation
PSDM	Participatory System Dynamics Modelling
RCM	Regional Climate Models
RCP	Representative Concentration Pathways
T	Temperature above surface
WCRP	World Climate Research Program
WEF	Water, Energy, Food

List of Tables

List of Figures

Executive Summary

The thorough analysis of the Water-Food-Energy and Climate nexus not only needs to account for the interactions taking place today, but also to consider how future climate will affect the three sectors in isolation or in combination (e.g. compounding/cascade effects). As such, climate projections for different climatic variables are necessary. This deliverable is aimed to provide the REXUS project partners (scientific and pilot teams) as well as the broader project stakeholders with critical information on the expected changes in the main climate variables for the project pilot areas. For the projection of future climate, a multi-model ensemble approach is adopted based on the ensemble mean of global and regional climate models. The climate variables examined are the mean temperature, total precipitation and potential evapotranspiration based on two Representative Concentration Pathways, the RCP4.5 and the RCP8.5, which are selected in order to represent an intermediate and a high emission scenario, respectively. The analysis takes place for the future period in three time steps (2031-2050, 2051-2070, 2071-2090), while the period 1986-2005 is used as the reference period. The climatic projections are carried out for the five REXUS pilot cases, namely the Pinios river basin (Greece), peninsular Spain, lower Danube river basin (Romania-Serbia-Bulgaria), Isonzo-Soča river basin (Italy-Slovenia) and Nima-Amaime subwatershed (Colombia) pilots, while the outputs are presented with the use of maps, diagrams and tables.

From the analysis of climate projections, it is concluded that, on average, the mean temperature shows a significant increase in the future period (2031-2090) for both scenarios, as well as, for all pilot areas except for the Nima-Amaime subwatershed. According to the results, the average increase in mean temperature on a pilot area basis is expected to be up to +2.1°C based on the RCP4.5, while for the RCP8.5 it may reach up to +4°C. The maximum average increase is observed at the Pinios, the lower Danube and the Isonzo-Soča river basins (3.9-4°C) for the period 2071-2090. In the case of the Nima-Amaime subwatershed, the mean temperature is not expected to change significantly in the short-term. Additionally, the analysis showed that the highest temperature increase is expected to be experienced at the lowlands, whereas the mountainous areas are expected to be less affected.

With respect to precipitation, a decreasing trend is noted for all the pilots according to the two future scenarios, with the exception of the Isonzo-Soča river basin pilot, where the precipitation shows a small increasing trend of up to 5% in the period 2051-2070 based on RCP4.5, however, the ensemble spread of the models' projections is exceptionally wide indicating a higher uncertainty of the results. For the case of Pinios river basin and of the peninsular area of Spain, the average decrease in precipitation reaches up to 12% and 15% respectively, in the 2071-2090 period based on RCP8.5. For the case of the Nima-Amaime subwatershed, the projections show a wide range of precipitation volumes, with an average increase of precipitation up to 24% during the short-term period, while for the long-term period the projections among the scenarios diverge. In specific, an average increase of 9% is foreseen based on RCP4.5, while a substantially higher average decrease of 29% is foreseen based on RCP8.5. Lastly, the precipitation projections for the lower Danube river basin do not show any statistical significant trend. In general, it is observed that the decrease in precipitation is greater at the lowlands and not so intense at the mountains.

The outputs of climate projections for the variable of daily potential evapotranspiration have a similar profile with that of temperature, as increasing trends are observed at all pilot areas and for both future scenarios. The highest average increase in potential evapotranspiration is observed during May-July for all pilots, apart from the case of Nima-Amaime subwatershed, where the highest increase is observed during the months of September-October. The pilot area for which the higher average increase is foreseen is that of Nima-Amaime subwatershed (~35%) followed by that of the peninsular Spain (~27%), while in the other pilots a lower increase of about 8-12% is expected.

1 Introduction

The current report is entitled "Fit-for-Nexus climate projections" and is produced as Deliverable 3.9 under the Task 3.5 "Climate projections for Nexus" of WP3 "REXUS Observatory" of the REXUS project. Climate and climate change is strongly connected to the Water-Energy-Food systems as it provides vital sources for their functionality and at the same time it may also have adverse effects on them. While energy generation and food production are both critical to society, they give rise to competing demands for water and are major contributors to negative water budgets, aquifer depletion and water quality degradation. Climate change can amplify these sectoral water demands while adding additional pressures on water resources and their management. Moreover, the evidence provided by modelled assessments of future climate impact on flooding is fundamental to water resources and flood risk decision making. Water resource availability is affected by altered precipitation patterns and increased rates of evaporation. Rainfed farming is expected to become more precarious at the mid and low latitudes, while productivity may rise at the higher latitudes. Apart from the impacts of reduced water availability and flooding on agriculture, climate may also affect crops through heat stress, frost or through a shift in sowing and harvesting dates (Shah et al., 2021; Liu et al., 2021; Fatima et al., 2020; Raza et al.,2019). The renewable energy potential is also inextricably linked to climate, with the hydropower generation potential already experiencing significant climate change impacts due to frequent and more pronounced droughts (Turral et al., 2011).

1.1 Relation to other Work Packages of REXUS

The main goal of the REXUS project is to provide tools, methods and demonstrating applications where regional, national and transboundary pilots manage their Nexus of Water, Energy, Food (WEF) systems and Climate in a way that interdependencies between the four are identified, well understood and taken into consideration. Five pilot areas have been selected to represent a wide spectrum of European and global Nexus situations, potentials, and implementation conditions. They span scales from sub-catchment (Pinios river, Greece; Lower Danube river, Romania-Serbia-Bulgaria) to tributary catchment (Nima river, Colombia) to full catchment (Isonzo-Soča river, Italy/Slovenia) and to national territory (peninsular Spain).

This deliverable is aimed to provide project partners (scientific and pilot teams) as well as the broader stakeholders with critical information on the expected changes in the main climate variables for the project pilot areas. This information can be used in sectoral or context specific analysis later on in the project, or even after the project end. In particular, the WP3 Tasks on Water and Energy accounting and footprints (Tasks 3.2-3.3) and on Land use mapping and EO indicators (Task 3.4), will use input generated from this Task (Task 3.5) to carry out their assessments for the future. Task 6.1 "Climate risk assessments in pilot cases" will make use of the results of this deliverable and contextualize them further through the production of context-driven climate risk indicators, i.e. climate indicators that will refer to specific risks on the WEF sectors as well as on the critical indicator thresholds set for each pilot area. Moreover, the results of this work will be used by the Participatory System Dynamics Modelling (PSDM) exercises of WP4 "Advancing Nexus Thinking" and WP6 "Pilot Implementation" to evaluate the role of different climate scenarios across the Nexus, through the analysis of nexus feedbacks for each pilot area.

1.2 Structure of the document

In the Section that follows (Section 2 Methodology), the methodology for carrying out the climate projections is laid down, including the selection of climate models, the climatic variables examined, the future scenarios, the timespan and the spatial resolution. In Section 3 "Outputs of climate projections for REXUS pilots", a description of each pilot area is provided, while next, the outputs of the climate projections for each climate variable and pilot area are presented in the form of maps, diagrams and tables, and discussed. The last Section of this document is the Conclusions section (Section 4) where the main findings of the analysis are summarized.

2 Methodology

Two types of models are used to produce climate projections, namely the Global Climate Models (GCMs) which simulate the climate at a global scale and the Regional Climate Models (RCMs) which simulate the climate only for a region. Climate models cover the globe in an imaginary grid. This grid mirrored many times, each above the other towards the edge of the atmosphere. The result can be imagined as many thousands of cubes on and above earth's surface and beneath the oceans. Then the current and future climate can be described in each of these cubes (Mc Sweeney & Hausfather, 2018).

GCMs, are numerical models with a typical spatial resolution ranging from 100–300km and require large computational power and time. On the contrary, RCMs have a higher resolution and cover a specific spatial domain of the globe. RCMs consider more detailed specifications of land use and water bodies, such us mountain's impact to the atmosphere system, simulate mesoscale processes in more detail than a GCM, because of the low resolution (Rummukainen, 2010).

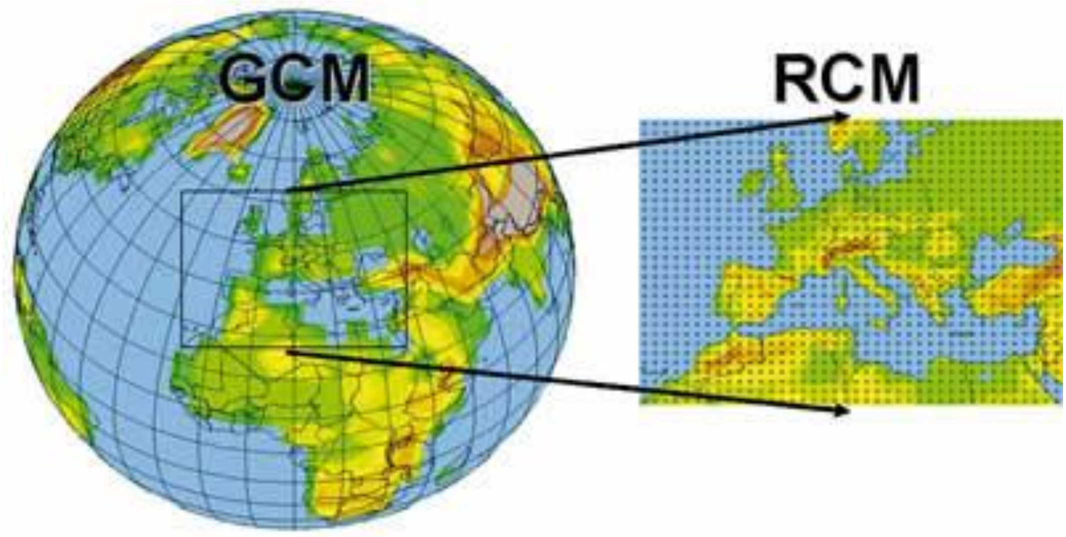

Figure 1: An RCM domain embedded in a GCM grid.

The data used in the following analysis were retrieved from the Copernicus Climate Change Service (C3S, 2019) and the Earth System Grid Federation (ESGF,2019). More specifically, the dataset was the outcome of the Coordinated Regional Climate Downscaling Experiment (CORDEX) database. CORDEX is a framework, under the World Climate Research Program (WCRP), to evaluate regional climate model performance through a set of experiments aiming at producing regional climate projections (Giorgi et al., 2009).

The examined climate variables are the mean temperature (T), precipitation (Prec) and potential evapotranspiration (ET). As for mean temperature, the data represents the mean ambient air temperature at 2m above the surface and the initial unit of the variable was Kelvin (°K), nevertheless a unit conversion has been applied to Celsius (°C). With respect to precipitation, the variable of the precipitation flux is used, after a conversion tomm$\cdot s^{-1}$. Potential evapotranspiration is defined as the amount of evaporation that would occur if a sufficient water source was available. The unit of the variable was (kg·m^2)/s^2, but a conversion tomm·s^{-1} was applied as well.

As for the spatial resolution of the datasets, the best available resolution was chosen, i.e. 0.11° (about 12km) for the European pilot areas (Spain, Danube, Isonzo, Pinios) and 0.20° (about 22.2km) for the South America domain, with the exception of potential evapotranspiration where the spatial resolution is lower (0.44° or about 48.8km). This resolution is deemed sufficient for the purposes of the present deliverable. Table 1 presents a list of the pilot areas with their coordinates and the spatial resolution provided in the analysis.

Table 1: Pilot area description by coordinates and resolution

Pilot area name	Country	Coordinates	Spatial resolution
Isonzo-Soča River Basin	Italy-Slovenia	46.49°N, 45.71°N, 12.94°E, 14.40°E	0.11°
Lower Danube River Basin	Romania, Bulgaria & Serbia	46.3°N, 41.85°N, 20.75°E, 30.66°E	0.11°
Nima-Amaime Subwatershed	Colombia	3.37°N, 3.81°N, 76.64°W, 75.94°W	0.20° & 0.44°
Pinios River Basin	Greece	40.24°N, 39.0°N, 21.44°E, 23.2°E	0.11°
Peninsular Spain	Spain	44.21°N, 35.82°N, 10.48°W, 4.3°E	0.11°

In the present study, the multi-model ensemble approach presented in the AR4 of the IPCC (Meehl et al. 2007) is adopted. In specific, an ensemble of five different Regional Climate Models (RCMs) that are driven by 5 different Global Climate Models (GCMs) is used. However, in cases where less models were available for a certain variable, a smaller number of model simulations has been used. In particular, for the case of south America, an ensemble of the two available models was selected for the variables of precipitation and temperature and an ensemble of three different models for the variable of potential evapotranspiration, due to lack of other simulations for the area. Detailed information on the climate models used is provided in Table 2. The selection of GCMs was based on the study of *McSweeney et al.* (2015), which illustrates a methodology for selecting among available models a set of GCMs for use in regional climate change assessments, based on their suitability across multiple regions. The selection of the RCMs was based on the studies of *Kotlarski et al.* (2014) and *Katragkou et al.* (2015) which provide a methodology for ensuring that the simulations selected are plausible and representative of future climate.

To identify whether the trends are due to a robust climate change signal and not the result of chance, trends are calculated for the statistical significance level of 0.05 (p-value≤0.05), according to the Mann-Kendall non-parametric test. The smaller the p-value, the stronger the evidence that you should reject the null hypothesis. There are two advantages of using this test. First, it is a non-parametric test and does not require the data to be normally distributed. Second, the test has low sensitivity to abrupt breaks due to inhomogeneous time series. According to this test, the null hypothesis H_0 assumes that there is no trend (the data is independent and randomly ordered) and this is tested against the alternative hypothesis H_1, which assumes that there is a trend

(Tabari et al., 2011). Mann Kendall test is a statistical test widely used for the analysis of trend in climatologic time series (Mavromatis & Stathis, 2011).

Table 2: Ensemble of models used for each climatic variable and area under study

Domain	Models		Variables		
	Global Climate Models (GCMs)	Regional Climate Models (RCMs)	Mean Temperature	Total Precipitation	Potential Evapotranspiration
EUROPE	ICHEC-EC-EARTH	KNMI-RACMO22E	✓	✓	-
	MOHC-HadGEM2-ES	CLMcom-CLM-CCLM4-8-17	✓	✓	-
	MOHC-HadGEM2-ES	KNMI-RACMO22E	✓	✓	✓
	MOHC-HadGEM2-ES	SMHI-RCA4	✓	✓	✓
	MPI-M-MPI-ESM-LR	CLMcom-CLM-CCLM4-8-17	✓	✓	-
	MPI-M-MPI-ESM-LR	MPI-CSC-REMO2009	✓	✓	✓
	MPI-M-MPI-ESM-LR	SMHI-RCA4	✓	✓	✓
	NCC-NorESM1-M	DMI-HIRHAM5	✓	✓	✓
	IPSL-CM5A-MR	SMHI-RCA4	✓	✓	✓
SOUTH AMERICA	CCCma-CanESM2	INPE-Eta	✓	✓	-
	MOHC-HadGEM2-ES	INPE-Eta	✓	✓	-
	CCCma-CanESM2	SMHI-RCA4	-	-	✓
	MOHC-HadGEM2-ES	SMHI-RCA4	-	-	✓
	MPI-M-MPI-ESM-LR	SMHI-RCA4	-	-	✓

The analysis is conducted on an annual basis for the variables of mean temperature and precipitation and on a seasonal basis for the daily potential evapotranspiration, in order to better capture the seasonality of the variable.

The analysis is conducted for two periods, the reference period from 1986 to 2005 and a future period from 2031 to 2090. For the future period, the analysis took place based on two Representative Concentration Pathways (RCPs). The RCPs describe four different 21st century pathways of greenhouse gas (GHG) emissions and atmospheric concentrations, air pollutant emissions and land use (IPCC, 2014). Among the four RCPs, RCP2.6 represents a stringent mitigation scenario (Van Vuuren et al., 2011), RCP4.5 and RCP6.0 are two intermediate scenarios (Thomson et al., 2011& Masui et al., 2011) and RCP8.5 is a scenario with very high GHG emissions (Riahi et al., 2011). The scenarios which do not assume additional efforts to constrain emissions ('baseline scenarios') lead to pathways ranging between RCP6.0 and RCP8.5. For the current analysis, the RCP4.5 and RCP8.5 were selected, the former serving for examining a more realistic mitigation scenario (compared to RCP2.6) and the latter representing a business-as-usual scenario where there is absence or lack of implementation of a GHG mitigation policy. Furthermore, the RCP4.5 is the only intermediate scenario for which there is data from the latest framework of the WCRP, CORDEX. In specific,

- RCP4.5 is a scenario that assumes stabilization of radiative forcing at 4.5 W/m^2 in the year 2100 without ever exceeding that value (intermediate mitigation scenario).
- RCP8.5 assumes that radiative forcing will exceed 8.5 W/m^2 by 2100 and will continue to rise for some amount of time (business-as-usual/ high GHG emissions scenario).

It is important to mention that there is a variety of uncertainty sources in climate projections, such as, model uncertainty, sampling uncertainty and scenario uncertainty. To address the uncertainty due to climate model selection, an ensemble of climate models is utilized, as the ensemble average usually tends to perform better than individual model runs (Wilcke & Bärring, 2016; IPCC, 2007; Reifen et al., 2009). Sampling uncertainty practically entails the uncertainties in statistics due to limited data while model uncertainty refers to low resolution of available spatial data, incorrectly simulating features of the climate system. Scenario uncertainty is the imperfect knowledge about the socio-economic and technological developments in the future, resulting in different emissions causing the emission of greenhouse gasses and the natural variability or internal variability of the climate system (e.g., solar intensity, volcanic eruptions, El Niño/La Niña) (Tebaldi & Knutti, 2007).

The outputs of the climate projections for the RCP4.5 and RCP8.5 are presented with the use of maps, diagrams and tables, in the section that follows (Section 3). In particular, the outputs for each climate variable and pilot area are presented as follows.

- Maps showing the spatial distribution of the values of the climatic variables for the reference period and the future period (2031-2090).
- Graphs with time series of the average values of the climate variables for the whole pilot area, together with the model ensemble's spread, i.e. the range of values provided by the projections of the different models. The time series are provided on an annual basis for the case of average temperature and total precipitation and on a monthly basis for the case of daily mean potential evapotranspiration.
- Tables providing the absolute values of the examined climate variables for the reference period and three 20-year future periods (2031-2050, 2051-2070, 2071-2090), as well as the relative change compared to the reference period. The three future periods are considered to represent the near-, mid- and long-term future, while the sub-division was made in 20-year intervals, similar to the reference period.

3 Outputs of climate projections for REXUS pilots

In this section, the results of the climate projections are provided for the examined climate variables and pilot areas of the project. The Section is broken down into individual sub-sections for each pilot area, where in each sub-section, a brief description of the pilot areas is firstly made, while next, the results of the climate projections are presented.

3.1 Pinios River Basin

3.1.1 Pilot area description

The Pinios river basin consists of two sub-catchments covering a total area of 11,000km² and is located at the Thessaly river basin District of Central Greece. The Pinios river is the third longest river of Greece, as it drains the entire drainage basin of Thessaly, part of which is the largest plain of the country. As about topography, the area is surrounded by mountains from 1,548m to 2,917m altitude, at its north and north-western areas. At the central and southern regions of the catchment, there is a flatter, agricultural land, where the altitude is less than 100m and at the coast is close to 0m.

The main economic activities present in the area are related to agriculture, tourism, livestock and fisheries. In particular, more than 50% of Thessaly is covered by agricultural land (51.7%), which makes Pinios river basin one of the most intensively cultivated and productive agricultural areas of Greece. The other main land uses are urban areas (2.5%) and forest (45%). Agricultural activity uses 96% of the water supply and is the main cause of significant water quantity and quality problems.

Two climate types are identified at Pinios river basin: continental climate conditions are dominant at the central and western part of Pinios river basin, while typical Mediterranean climate conditions are met at the eastern part. Additionally, during the summer period (June to August) precipitation is rare for the whole Pinios river basin (Psomas et al., 2016). The highest temperature is observed at the center of the basin where there is arable land and urban areas, while towards the mountains the temperature is significantly lower.

In the following maps, the topography and location of the pilot area, as well as, the main land uses/land covers are provided.

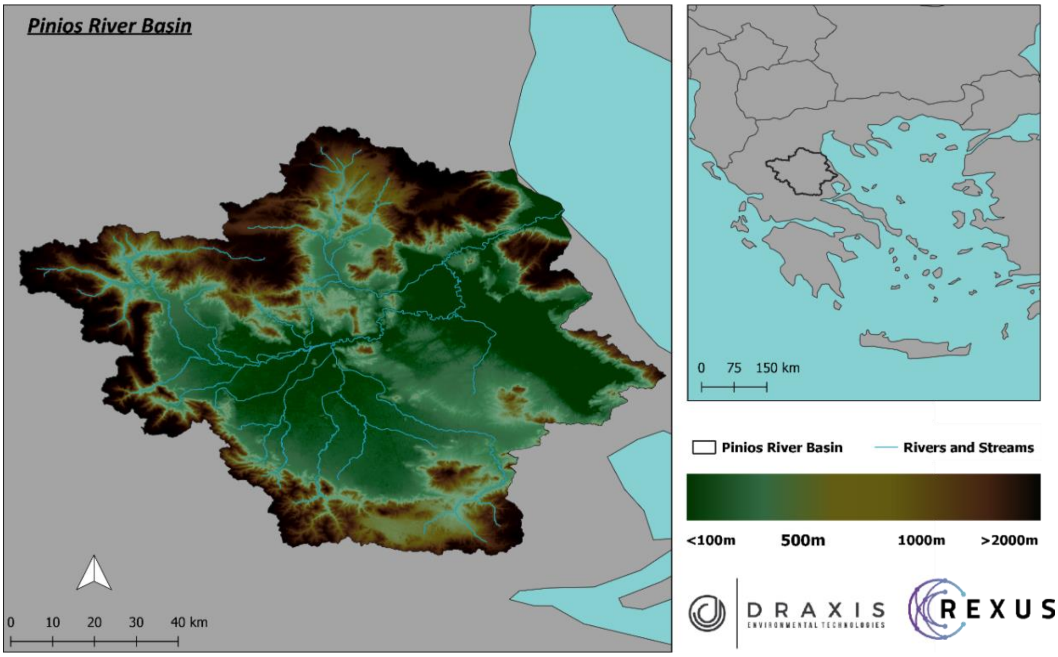

Figure 2: Topographic map of the Pinios river basin.

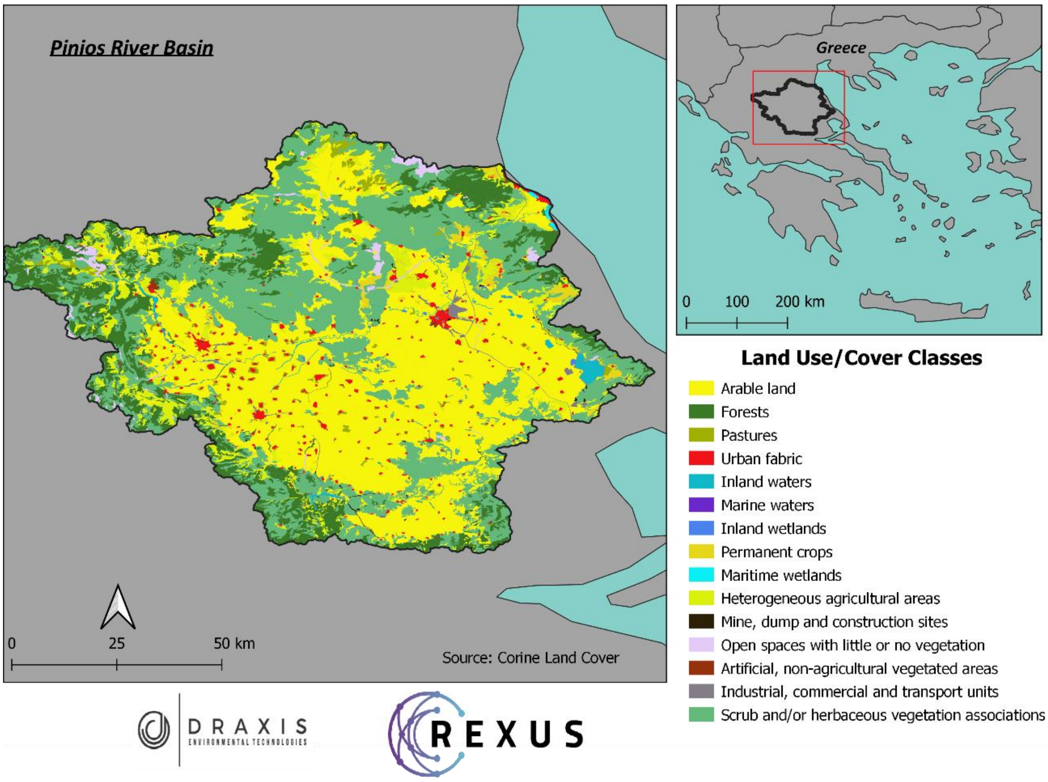

Figure 3: Land use/Land cover map of the Pinios river basin.

3.1.2 Climate projections

Temperature

The projected ensemble annual mean temperature for the period 2031-2090, at Pinios River Basin, is presented in the form of time series, in Figure 4. As it may be observed, there is a clear tendency for temperature increase during the future 60-year period according to both scenarios. Additionally, the mean temperature for both scenarios is above 14°C for the whole period. Nevertheless, the ensemble spread for RCP4.5 extends to lower temperatures, especially during the period 2050-2055, when it reaches the minimum mean temperature of 11°C. The maximum value of annual mean temperature is observed in the case of the RCP8.5 ensemble spread and in specific during the last years of the time series when it reaches the value of 20-21°C.

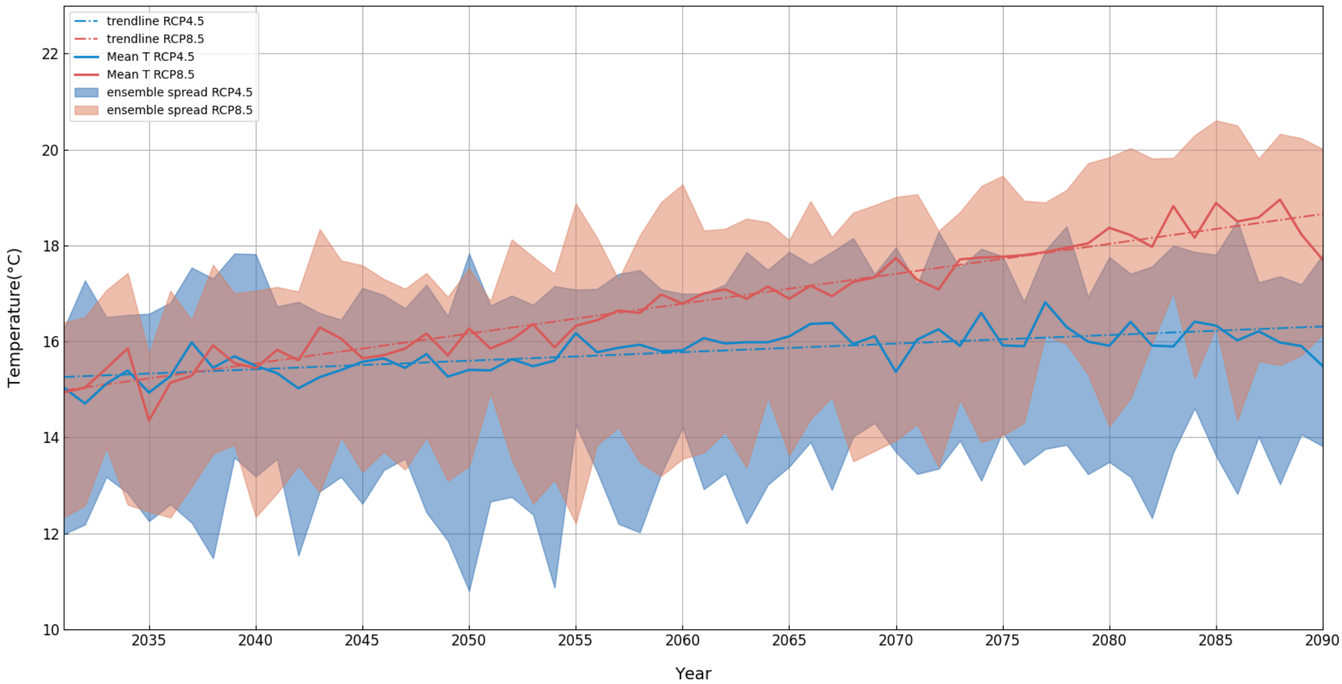

Figure 4: Ensemble mean of mean temperature of the period 2031-2090 for the RCP4.5 (blue line) and RCP8.5 (red line) and ensemble spread (coloured area), Pinios river basin.

The mean temperature of the examined reference and future periods along with the change compared to the reference period are shown in Table 3. It may be seen that for the near-term period (2031-2050) there is no significant difference between the two scenarios, however there is an increase in mean temperature of 1.3°C (+9%) and 1.6°C (+11%) for the RCP4.5 and RCP8.5 respectively, compared to the reference period. For the mid-term period (2051-2070) the warming trend is about 1.9°C (+14%) for the RCP4.5 and 2.8°C (+20%) for the RCP8.5. Finally, for the long-term period (2071-2090) the increase is 2.1°C (+15%) for the intermediate scenario (RCP4.5), while the high-emissions scenario (RCP8.5) predicts an increase of 4°C (+29%) at Pinios river basin.

Table 3: Ensemble mean temperature for the reference period and the future sub-periods based on the RCP4.5 and RCP8.5, Pinios river basin.

Temperature	Reference period	2031-2050		2051-2070		2071-2090	
		RCP4.5	RCP8.5	RCP4.5	RCP8.5	RCP4.5	RCP8.5
Absolute value (°C)	14	15.3	15.6	15.9	16.8	16.1	18
Change (°C)		+ 1.3	+ 1.6	+ 1.9	+ 2.8	+ 2.1	+ 4
Relative change (%)		+ 9	+ 11	+ 14	+ 20	+ 15	+ 29

Regarding the spatial distribution of mean temperature range as this is depicted in Figure 5, it is observed that during the reference period the mean temperature range starts below 8°C at the mountains and reaches up to 16-18°C at the lowlands at the center of the basin, where the agricultural lands are located. During the future period, the maximum mean temperatures remain similar to the reference period (16-18°C) for RCP4.5, however they are observed at a much greater area than the reference period. In addition, the respective minimum mean temperatures are increased up to 10°C. According to the scenario RCP8.5, the minimum mean temperatures at the mountains are expected to range between 10 and 12°C, while at the lowlands they expected to exceed 18°C, both at the centre of the basin and at the north-eastern part.

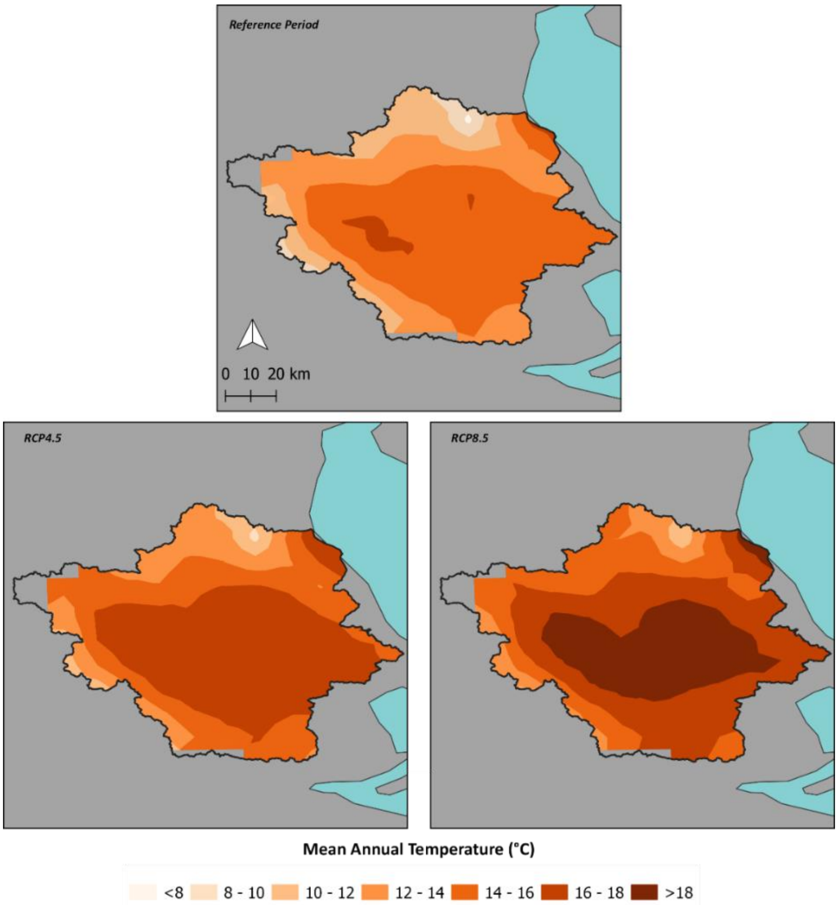

Figure 5: Spatial distribution of the mean annual temperature, for the reference period (top) and the future period based on the RCP4.5 and RCP8.5 (bottom), Pinios river basin.

Precipitation

The projected ensemble mean total precipitation for the period 2031 to 2090 for the two scenarios at Pinios river basin is presented in the form of annual time series in Figure 6. As it may be seen, total precipitation tends to decrease over the 60-year period for both scenarios. Moreover, the average precipitation is above 600mm during the whole period for the RCP4.5. With respect to RCP8.5, a differentiation is most clearly observed from the mid-term period and onwards.

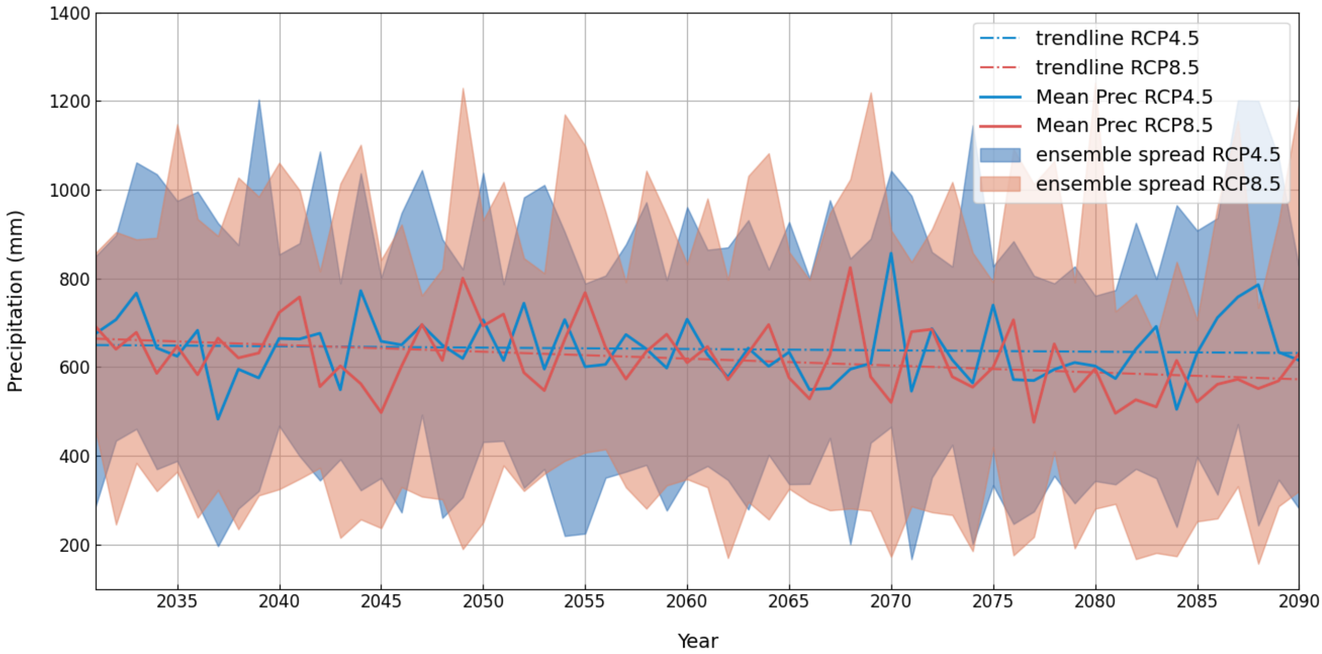

Figure 6: Ensemble mean of total precipitation of the period 2031-2090 for the RCP4.5 (blue line) and RCP8.5 (red line) and ensemble spread (coloured area), Pinios river basin.

In Table 4, the projected average annual total precipitation for the examined reference and future periods along with the relative change compared to the reference period is provided. It may be concluded that for the near-term period (2031-2050) there is no significant difference between the two scenarios and the reference period. For the mid-term period (2051-2070), the ensemble mean shows decreasing trends, about 23mm (-3%) for the RCP4.5 and 29mm (-4%) for the RCP8.5. Finally, for the long-term period (2071-2090) the decrease is 27mm for the intermediate scenario, while for the high emissions scenario the difference is more pronounced, reaching -78mm.

Table 4: Ensemble mean of total precipitation, for the reference period and the future sub-periods based on the RCP4.5 and RCP8.5, Pinios river basin.

Precipitation	Reference period	2031-2050		2051-2070		2071-2090	
		RCP4.5	RCP8.5	RCP4.5	RCP8.5	RCP4.5	RCP8.5
Absolute value (mm)	660	653	643	637	631	633	581
Change (mm)		-7	-17	-23	-29	-27	-78
Relative change (%)		-1	-3	-3	-4	-4	-12

Proceeding to the geospatial variation of the precipitation for the different scenarios as this is depicted in Figure 7, it may be said that the most significant change appears at the mountain Olympus, at the North part of the basin, where precipitation decreases compared to the reference period, especially for RCP8.5. As it may be seen, the maximum average annual total precipitation for RCP8.5 does not exceed 2500mm, in contrast to the reference scenario and RCP4.5.

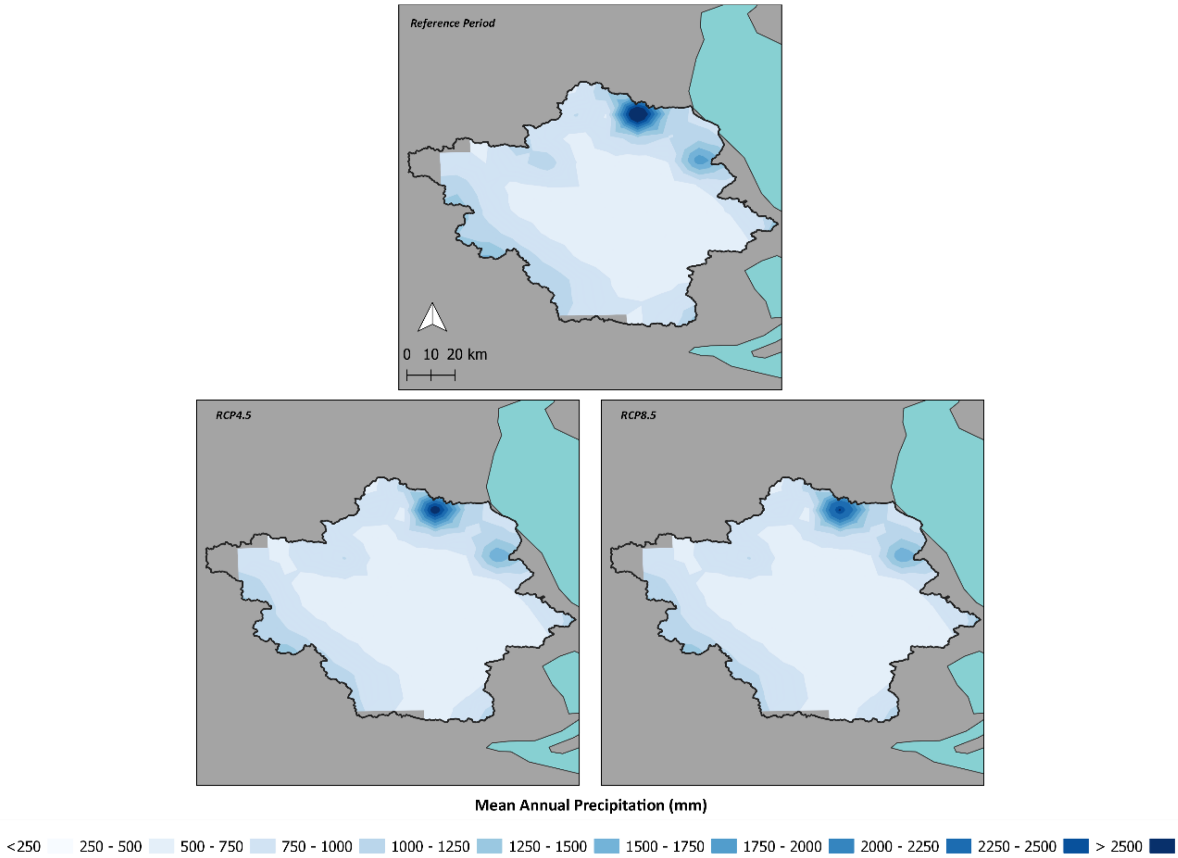

Figure 7: Spatial distribution of the mean annual total precipitation for the reference period (top) and the future period based on the RCP4.5 and RCP8.5 (bottom), Pinios river basin

Potential Evapotranspiration

The projected ensemble mean of the mean daily potential evapotranspiration on a monthly basis is presented in Figure 8, in the form of time series for the period 2031-2090. As it may be seen in the following diagram, the maximum values are observed during the summer months (from May to August) with the absolute maximum, during July, with approximately 11% relative change, compared to the reference period. On the other hand, the minimum values are observed during the winter months, with the absolute minimum, in December. Both RCPs show increasing trends in daily mean values for all months for the period 2031-2090, in comparison to the reference period. The potential evapotranspiration values for RCP8.5 are higher compared to RCP4.5 which is expected as the variable follows a very similar pattern to that of temperature. The largest increase in potential evapotranspiration compared to the reference period is observed during the months of May, June and July.

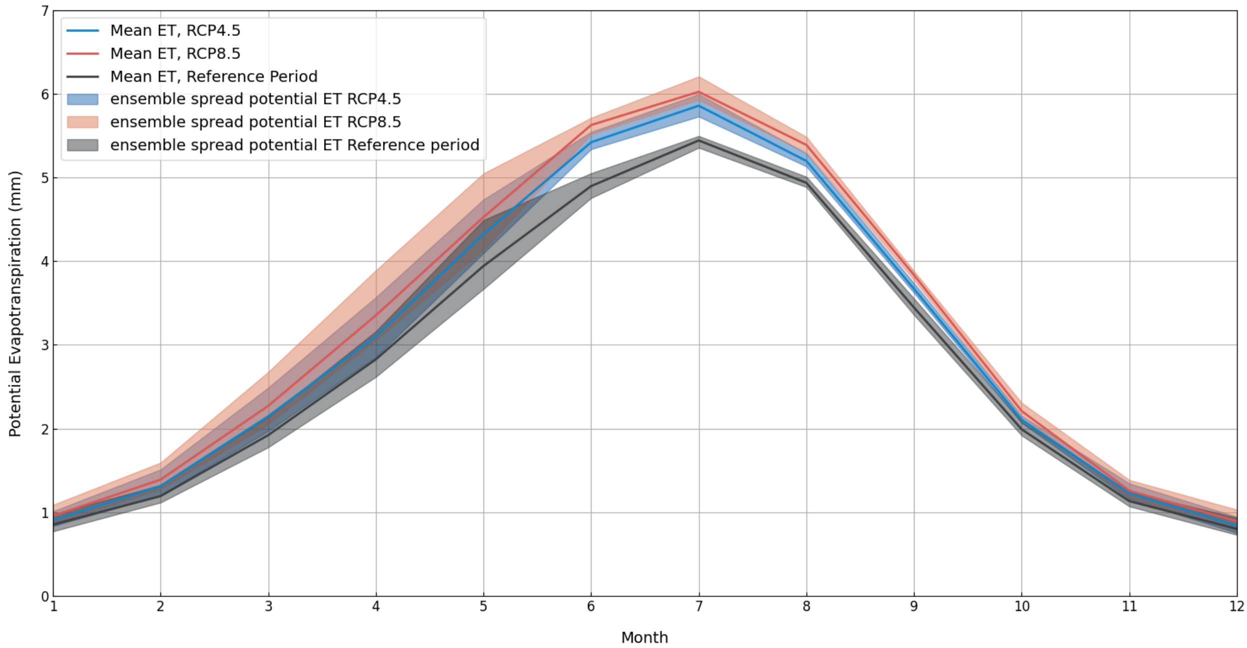

Figure 8: Ensemble mean of the mean daily potential evapotranspiration per month, of the period 2031-2090 for the RCP4.5 (blue line) and RCP8.5 (red line) as well as the reference period 1986-2005 (grey line) and ensemble spread (coloured area), Pinios river basin.

Regarding the spatial distribution of the mean daily potential evapotranspiration range as this is depicted in Figure 9, it is observed that during the reference period the mean daily potential evapotranspiration range starts from 2 to 2.5mm at the mountains and reaches up to 3.5-4mm at the lowlands. The potential evapotranspiration presenting increasing trends for the future period (for both scenarios), in comparison with the reference period. As it is shown, during the future period, the maximum mean daily potential evapotranspiration is increasing up to 4.5mm for RCP4.5, however it is observed only in a small area. For the RCP8.5, values from 4 to 4.5mm are observed at a much greater area.

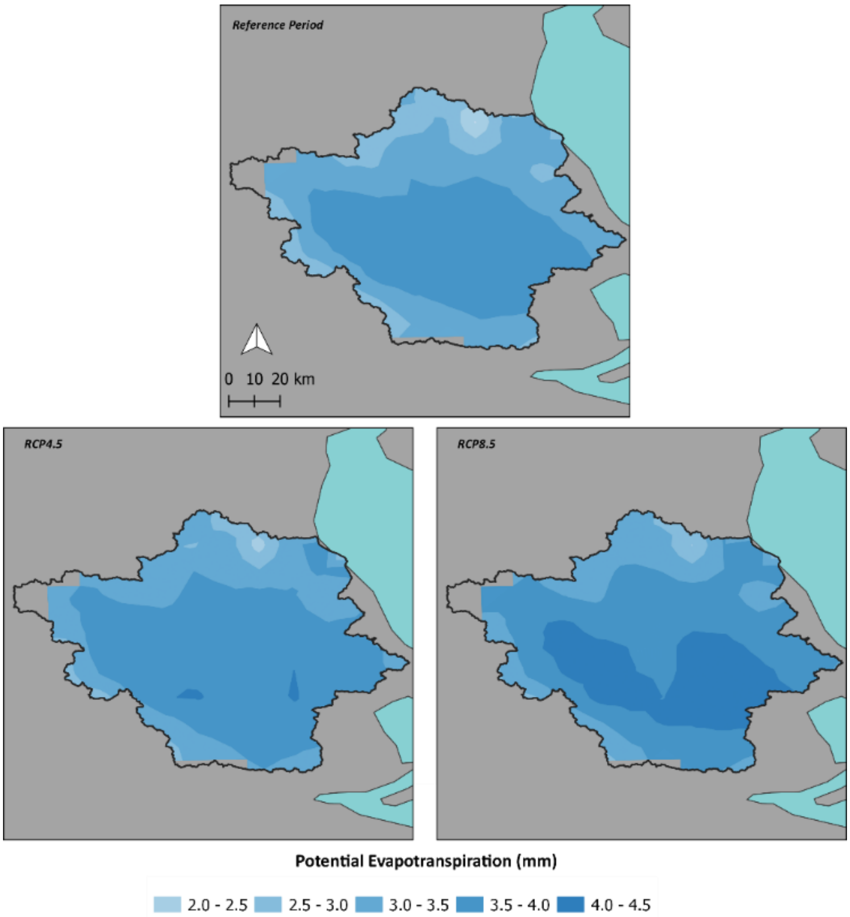

Figure 9: Spatial distribution of the mean daily potential evapotranspiration, for the reference period (top) and the future period based on the RCP4.5 and RCP8.5 (bottom), Pinios river basin.

3.2 Peninsular Spain

3.2.1 Pilot area description

This pilot area covers the peninsular territory of Spain which is the fourth largest country in the European continent. Spain is located at the south-western part of Europe occupying about 82% of the Iberian Peninsula with a total area of 505,990km^2. The country has both lowlands and large mountain ranges, some of which have high altitudes. The country is crossed by five major mountain systems: Pyrenees, which form a natural frontier between Spain and France, Betic Mountain Ranges, along the southern and eastern parts of Spain, the Cantabrian Mountains, across northern Spain, including the highest mountain in the Iberian Peninsula "Mulhacén (3,479m)", the Meseta Central System, in the center of the peninsula and the Iberian System which extends from the eastern foothills of the Cantabrian Mountains to the Betic System (del Rio et al., 2011). The Spanish mainland is bordered to the south and east almost entirely by the Mediterranean Sea, to the north by France, Andorra, and the Cantabrian Sea; and to the west by the Atlantic Ocean and Portugal. Water resources in Spain are managed by autonomous communities and river basin districts, the latter having the competency for the design, planning, and supervision on the use of these resources. The country has over 1,800 rivers and streams, however only the Tagus is more than 960km long. The major rivers flowing westward through the Meseta Central include the Duero, the Tagus, the Guadiana, and the Guadalquivir rivers (REXUS, 2021).

Due to its complex orography and geographic location, Spain has great climatic variability. Interannual climatic variability is high and is conditioned to a great extent, specifically with respect to precipitation, by atmospheric circulation patterns in the Northern hemisphere, in particular by the North Atlantic oscillation (Moreno et al., 2005).

In the following maps, the topography and location of the pilot area, as well as, the main land uses/land covers are provided.

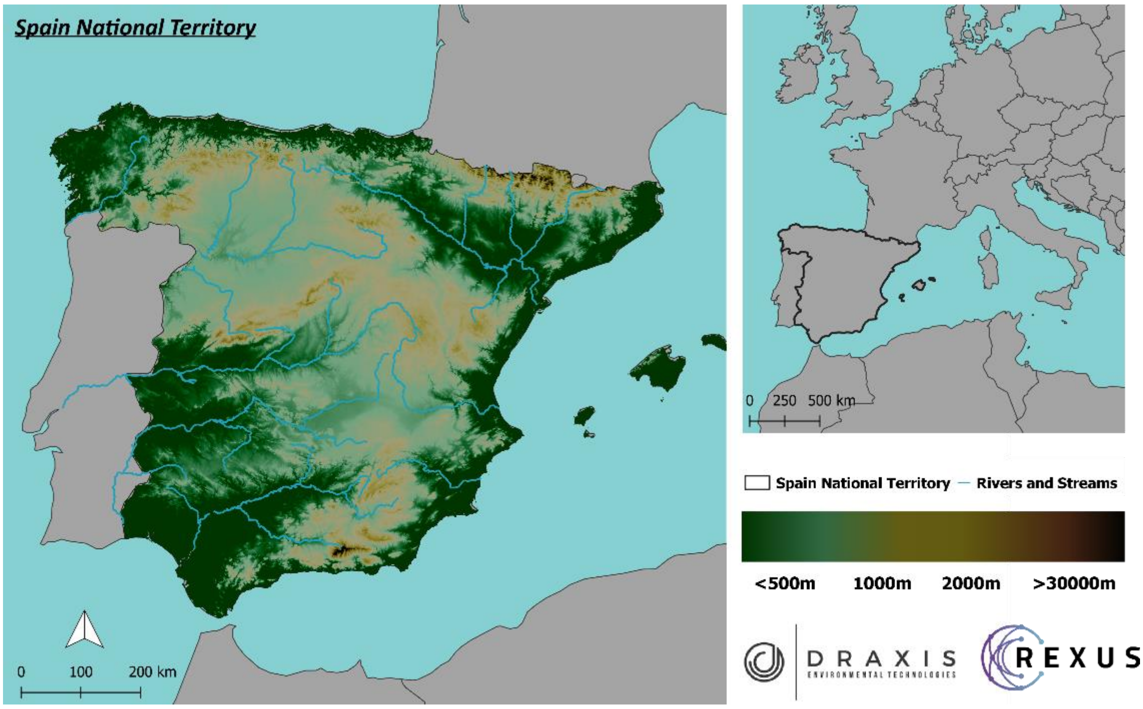

Figure 10: Topographic map of Spain

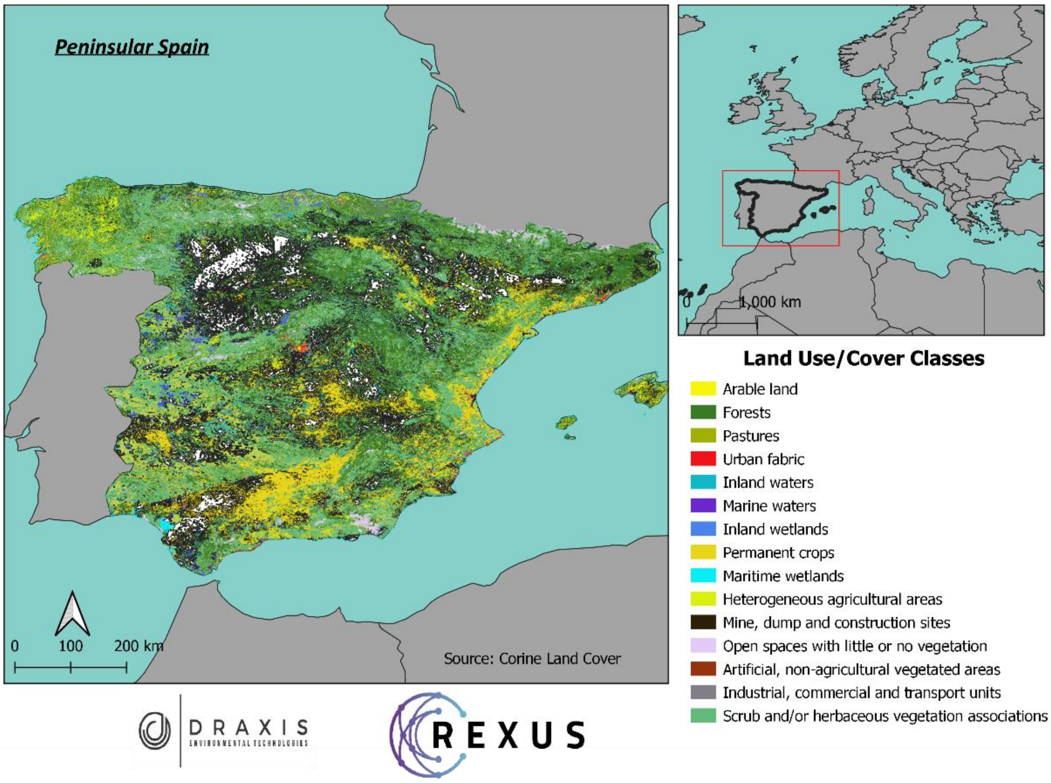

Figure 11: Land use/Land cover map of the peninsular Spain.

3.2.2 Climate Projections

Temperature

The projected ensemble annual mean temperature during the period 2031-2090 for the pilot area of peninsular Spain is presented in the form of time series in Figure 12. As it may be observed, there is a clear tendency for temperature increase during the future 60-year period according to both scenarios. Moreover, the mean temperature is above 15.5°C during the whole period for both scenarios. Nevertheless, the ensemble spread for RCP4.5 extends to lower temperatures. The maximum annual mean temperature is observed in the case of the RCP8.5 ensemble spread and in specific during the last years of the time series, when it reaches the value of 21°C.

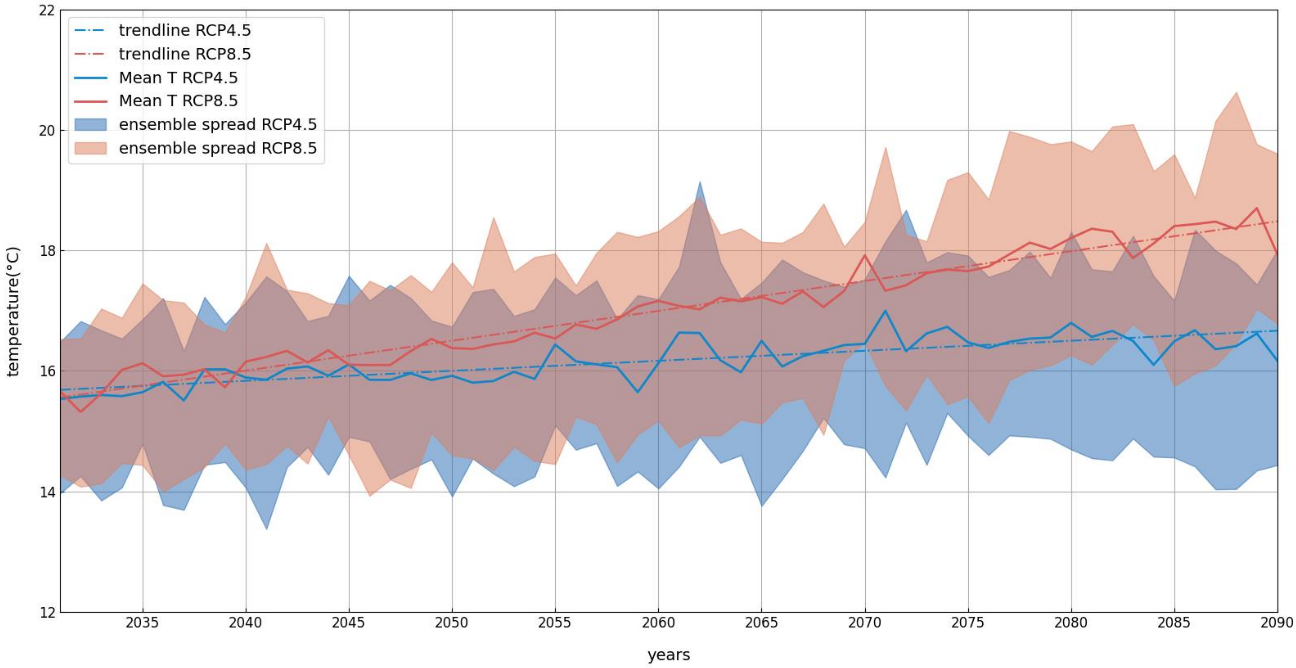

Figure 12: Ensemble mean of mean temperature of the period 2031-2090 for the RCP4.5 (blue line) and RCP8.5 (red line) and ensemble spread (coloured area), Spain.

The projected mean annual temperature for the reference and the future sub-periods along with the respective change is summarized in Table 5. As it may be seen, there is no significant difference between the two scenarios for the near-term period (2031-2050) compared to the reference period, with a projected increase in mean temperature of 1.1-1.3°C on average. For the mid-term period (2051-2070), the expected increase in mean annual temperature is up to 1.5°C for the RCP4.5 and 2.3°C for the RCP8.5. Finally, for the long-term period (2071-2090), the increase is expected to reach 1.8°C for the intermediate scenario (RCP4.5) and 3.3°C for the high-emissions scenario (RCP8.5).

Table 5: Ensemble mean temperature for the reference period and the future sub-periods based on the RCP4.5 and RCP8.5, Spain.

Temperature	Reference period	2031-2050		2051-2070		2071-2090	
		RCP4.5	RCP8.5	RCP4.5	RCP8.5	RCP4.5	RCP8.5
Absolute value (°C)	14.7	15.8	16	16.2	17	16.5	18
Change (°C)		+ 1.1	+ 1.3	+ 1.5	+ 2.3	+ 1.8	+ 3.3
Relative change (%)		+ 7	+ 9	+ 10	+ 16	+ 12	+ 22

The spatial distribution of mean temperature range is depicted in Figure 13. It is observed that during the reference period the mean temperature range starts below 2°C at the mountains and reaches up to 20°C at the lowlands. As it may be seen, the largest increase in mean temperature is observed at the south-western part of Spain for both scenarios during the period 2031-2090. More specifically, at the south-western part of Spain, the area projected to experience an increase in mean temperature up to 20°C, is expected to be significantly expanded compared to the reference period according to RCP4.5. Similarly, a considerable part of this area is expected to experience a mean temperature of over 20°C according to RCP8.5. Additionally, a higher increase in mean temperature is expected at the areas surrounding the large cities of Spain, such as Saragossa, Barcelona, and Seville while the increase at the mountainous areas are lower for both scenarios, compared to the reference period.

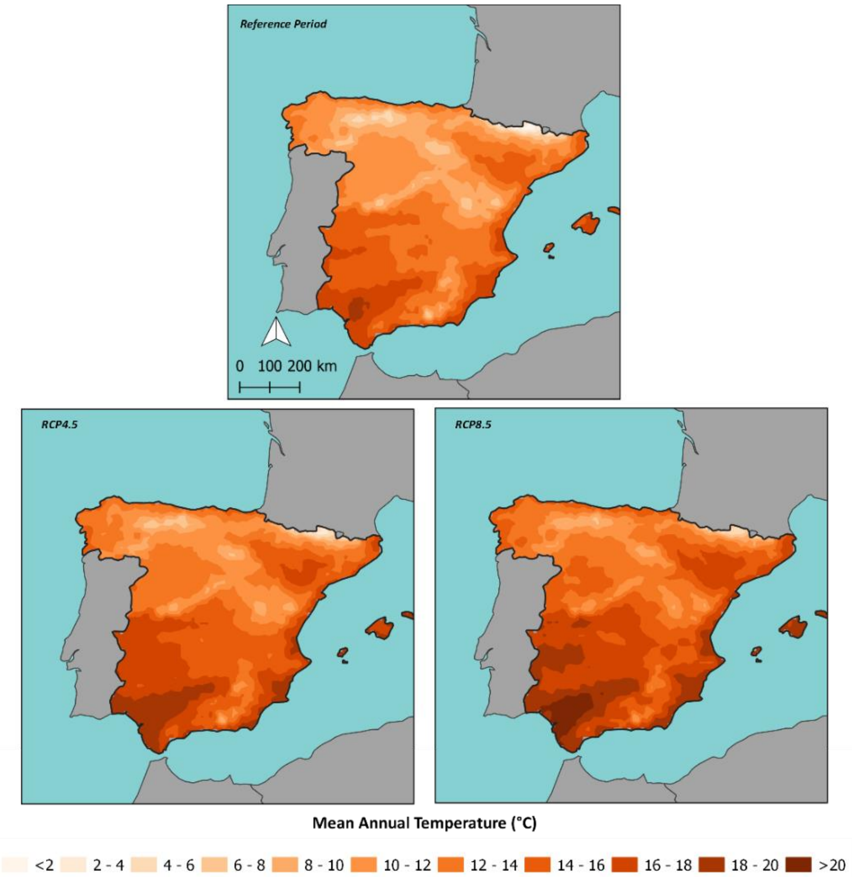

Figure 13: Spatial distribution of the mean annual temperature for the reference period (top) and the future period based on the RCP4.5 and RCP8.5 (bottom), Spain.

Precipitation

The projected ensemble mean total precipitation for the pilot of Spain based on the two scenarios is presented in Figure 14 in the form of annual time series for the period 2031 to 2090. As it may be seen, total precipitation tends to decrease over the 60-year period according to both scenarios. The average precipitation is above 600mm during the whole period for the RCP4.5, while a differentiation is observed in the respective values for RCP8.5 especially from the mid-term period and onwards, when there is a more obvious decreasing trend for the latter. The maximum value of annual total precipitation is observed in the case of the RCP4.5 ensemble spread and in specific during the first years of the time series when it reaches the value of 1200mm. The minimum annual precipitation value of the ensemble spread is about 300mm and is observed after the second half of the time series based on both scenarios.

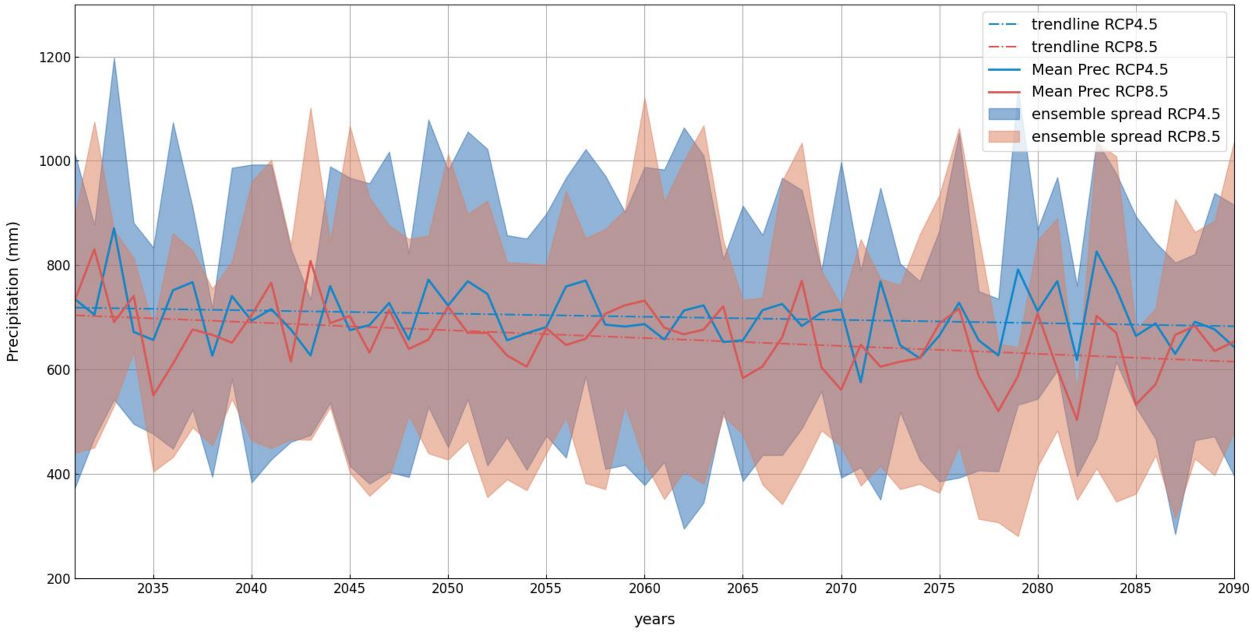

Figure 14: Ensemble mean of total precipitation of the period 2031-2090 for the RCP4.5 (blue line) and RCP8.5 (red line) and ensemble spread (coloured area), Spain.

In Table 6, the projected average annual total precipitation for the examined reference period as well as for the future sub-periods under examination, is provided. It may be concluded that for the near-term period (2031-2050), there is no significant difference between the two scenarios and the reference period. For the mid-term period (2051-2070), the ensemble mean precipitation shows a decreasing trend, about 36mm (-5%) for the RCP4.5 and 77mm (-10%) for the RCP8.5. Finally, for the long-term period (2071-2090) the decrease is 51mm (-7%) for the intermediate scenario, while for the high emissions scenario the difference is more pronounced, reaching -113mm (-15%).

Table 6: Ensemble mean of total precipitation, for the reference period and the future sub-periods based on the RCP4.5 and RCP8.5, Spain.

Precipitation	Reference period	2031-2050		2051-2070		2071-2090	
		RCP4.5	RCP8.5	RCP4.5	RCP8.5	RCP4.5	RCP8.5
Absolute value (mm)	739	712	690	703	663	688	626
Change (mm)		-27	-49	-36	-77	-51	-113
Relative change (%)		-4	-7	-5	-10	-7	-15

The geospatial distribution of the precipitation for the different scenarios is depicted in Figure 15. As it may be seen, there is a great spatial distribution of precipitation throughout the country. The maximum amount of precipitation is observed at the north-western part of the country, where the climate of the region is affected by the Atlantic Ocean, while the minimum amount is observed at the southern part of Spain. There is no significant difference between the two RCPs, however the differences in relation to the reference period are more noticeable at the eastern and central part of the country, for both scenarios. It is noteworthy that during the reference period, the maximum precipitation values exceed 3500mm, while in the future the respective values are not expected to exceed 3000-3500mm. In addition, the results show that a large part of the southern and eastern part of the country is expected to experience a reduction of precipitation to about 500mm, which is expected to be more widely felt in the case of RCP8.5.

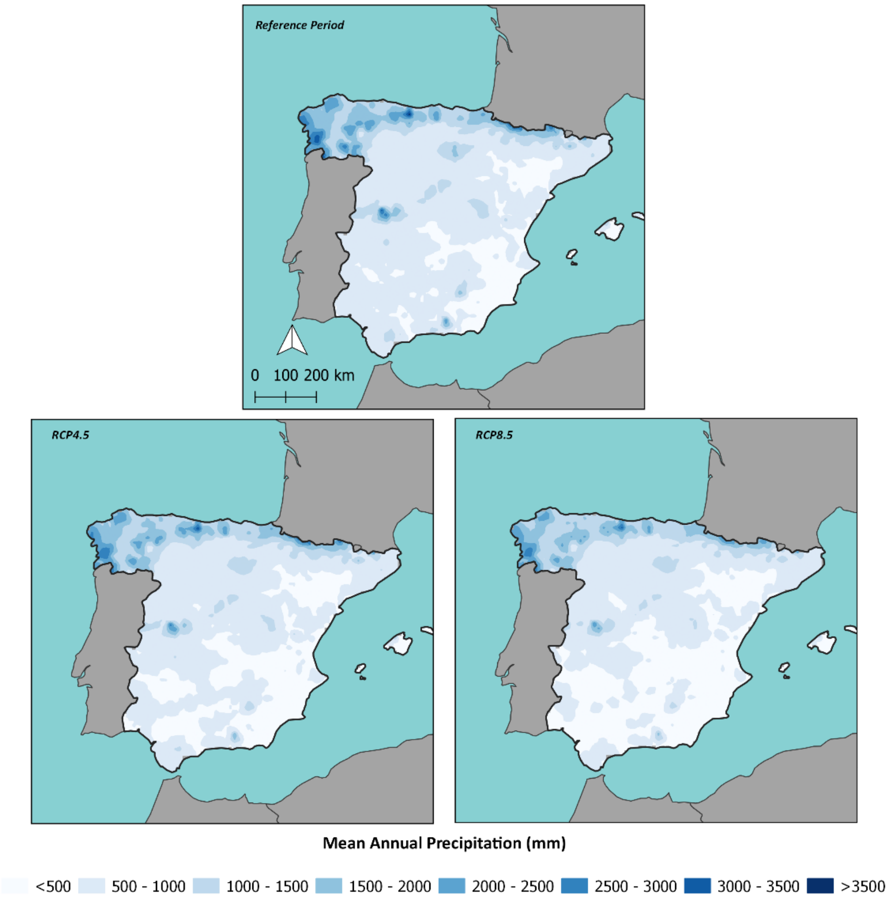

Figure 15: Spatial distribution of the mean annual total precipitation for the reference period (top) and the future period based on the RCP4.5 and RCP8.5 (bottom), Spain.

Potential Evapotranspiration

The projected ensemble mean of the mean daily potential evapotranspiration on a monthly basis is presented in Figure 16, in the form of time series for the period 2031-2090, for the pilot of Spain. As it may be seen, the maximum values are observed during July and the minimum values during December. Both RCPs show increasing trends in daily mean values for all months for the period 2031-2090, in comparison to the reference period. The potential evapotranspiration values for RCP8.5 are higher compared to RCP4.5 which is expected, as the variable follows a very similar pattern to that of temperature. The largest increase in potential evapotranspiration compared to the reference period is observed during April to September, with the months of May and June marking an increase of approximately 27%.

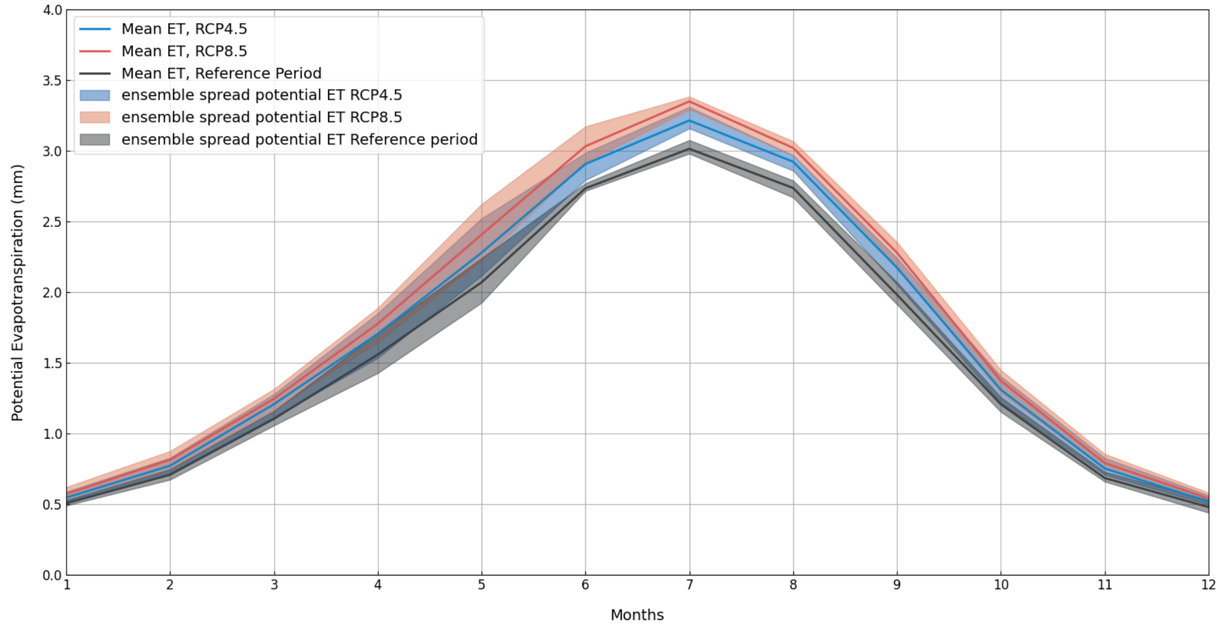

Figure 16: Ensemble mean of the mean daily potential evapotranspiration per month, of the period 2031-2090 for the RCP4.5 (blue line) and RCP8.5 (red line) as well as the reference period 1986-2005 (grey line) and ensemble spread (coloured area), Spain.

The spatial distribution of the mean daily potential evapotranspiration range is depicted in Figure 17. As it may be observed, during the reference period the mean daily potential evapotranspiration starts from less than 1.5mm at the mountains and reaches up to 4.5mm at the lowlands. During the future period, the maximum mean daily potential evapotranspiration remains similar to the reference period (4-4.5mm) based on RCP4.5, however this is observed at a much greater area compared to the reference period. For the RCP8.5, the maximum evapotranspiration values exceed 4.5mm.

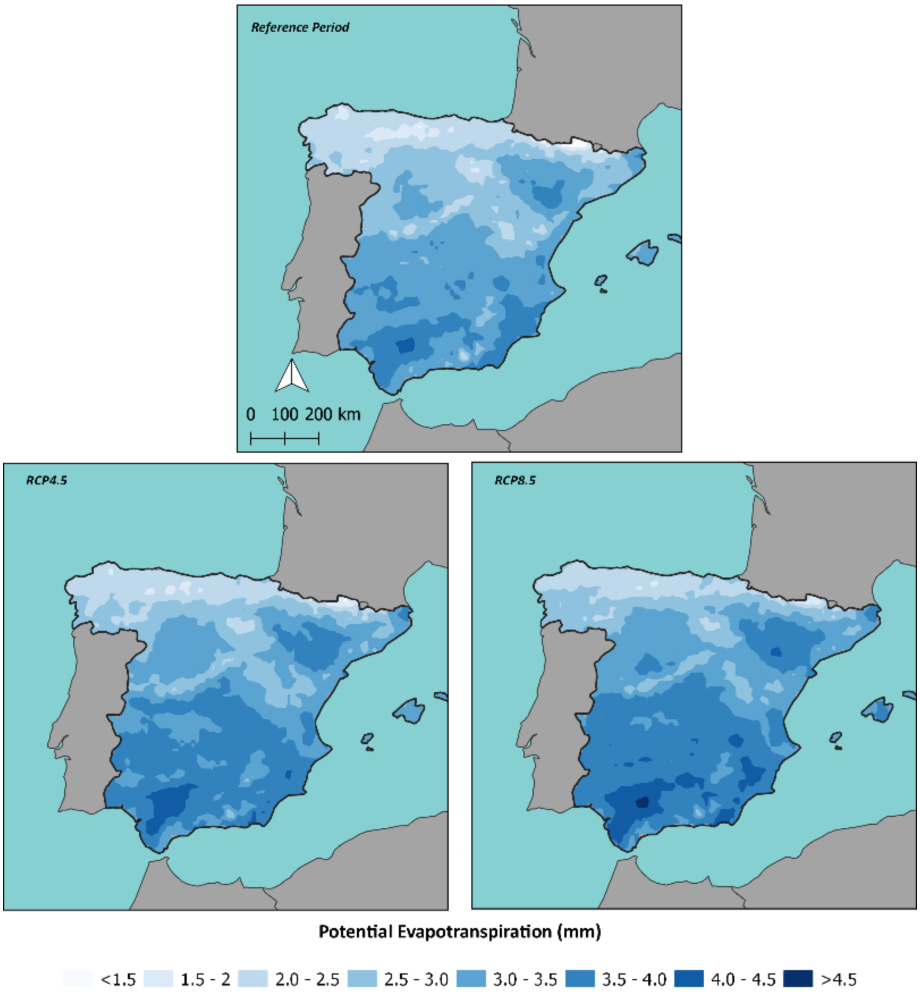

Figure 17: Spatial distribution of the mean daily potential evapotranspiration, for the reference period (top) and the future period based on the RCP4.5 and RCP8.5 (bottom), Spain.

3.3 Lower Danube River Basin

3.3.1 Pilot area description

The Danube river is the second-longest river in Europe, running through ten countries flowing for 2850km until it reaches the Black Sea. The Romanian section covers almost a third (29%) of the surface area of the river basin, and over a third of the river's length flows through the country. After squeezing through the Iron Gates gorge and dams between Serbia and Romania, the Danube flows free for 1000km through Romania, Bulgaria, Moldova and Ukraine before emptying into the Black Sea. The Lower Danube which is the study area of this project, is one of the last free flowing stretches of river in Europe. Dependent on this part of the river are not only some of Europe's greatest natural treasures, but also the 29 million people who live at the Lower Danube river basin – people who directly benefit from the many services that the river provides (WWF, 2015). The Lower Danube river basin experiences a temperate climate, with precipitation all year round, except for the summers, which are more hot and dry. Compared to the other regions of Romania, it experiences the highest temperatures, both in winter and in summer due to its location which is in the south and closer to areas characterized by the Mediterranean climate type. At the northern part of the study area, there is a very large part of the Carpathian Mountains, called the "Southern Carpathian Mountains, with the highest altitude reaching about 2544 m. The Balkan Mountains border the lower Danubian Plain on the south. Their rounded summits have an average height of 722 m and rise to 2376 m at Mount Botev, the highest peak (Danforth et al., 2021).

In the following maps, the topography and location of the pilot area, as well as, the main land uses/land covers are provided.

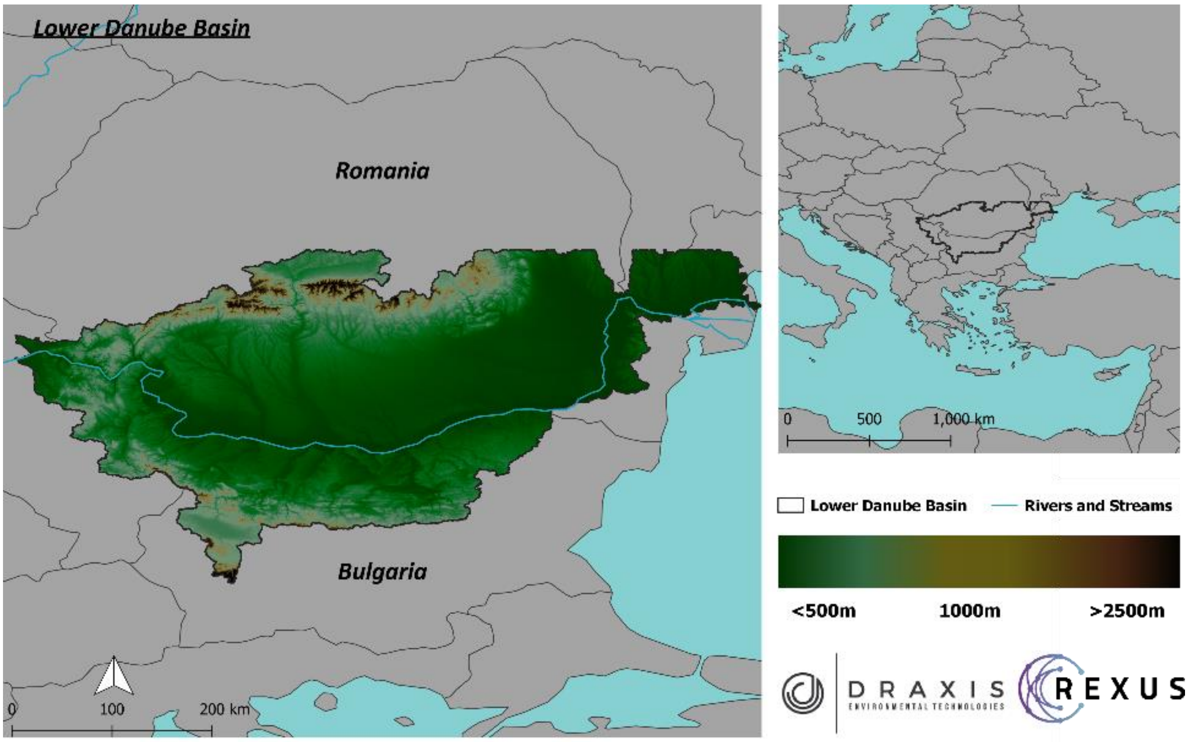

Figure 18: Topographic map of the Lower Danube river basin study area

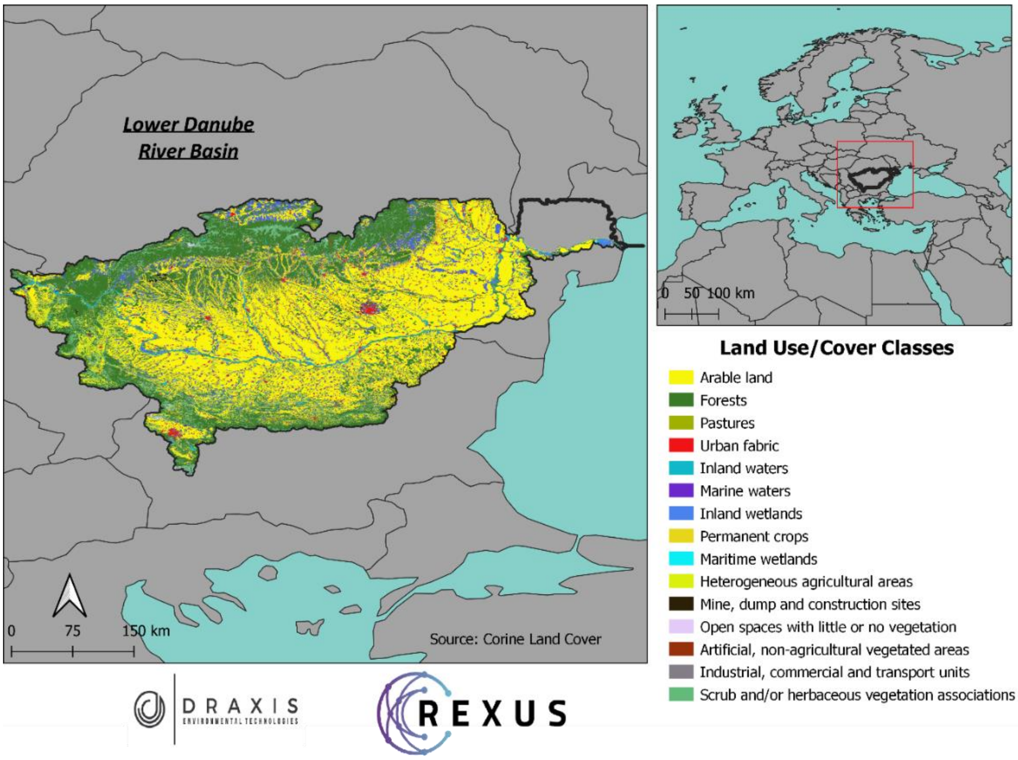

Figure 19: Land use/Land cover map for the lower Danube river basin.

3.3.2 Climate Projections

Temperature

The projected ensemble annual mean temperature for the period 2031-2090, for the lower Danube river basin, is presented in the form of time series in Figure 20. As it may be observed, there is a clear tendency for temperature increase during the future 60-year period in both scenarios, with the mean temperature being above 12°C for almost the whole period. A clear differentiation among the scenarios with more obvious increasing trends for the case of RCP8.5, is observed from 2050 and onwards. The maximum value on the ensemble spread is observed in the case of the RCP8.5 and in specific during the last years of the time series, when it exceeds the value of 17°C. On the other hand, the ensemble spread for RCP4.5 extends to lower temperatures, and it reaches the minimum mean temperature of 8.5°C during the period 2050-2055.

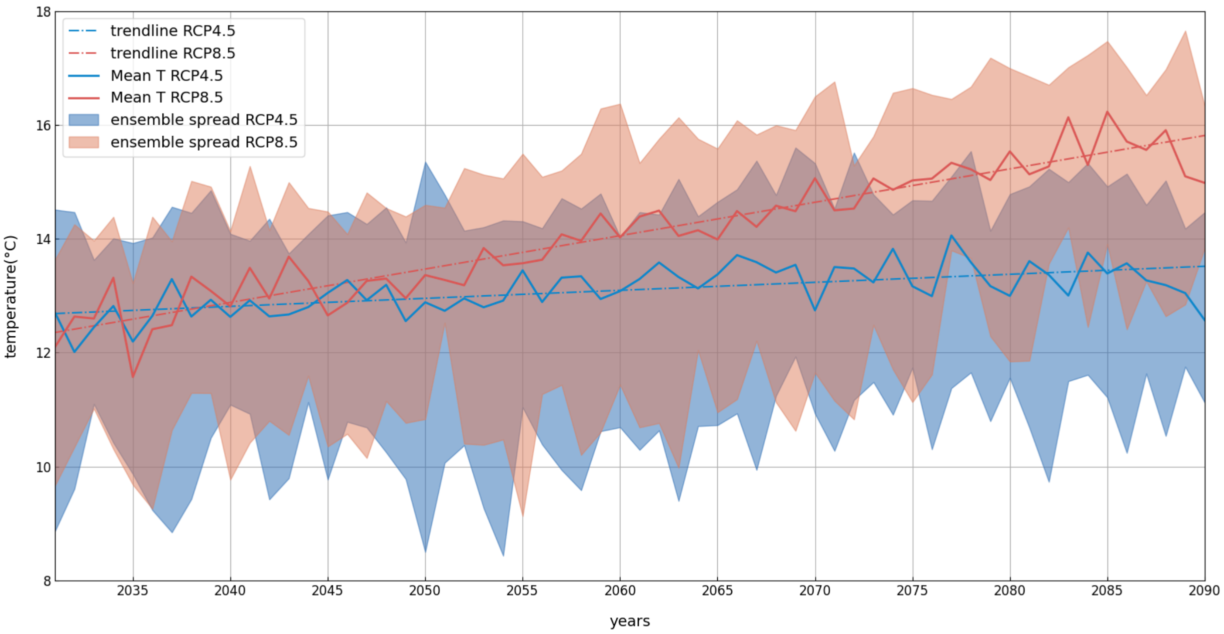

Figure 20: Ensemble mean of mean temperature of the period 2031-2090 for the RCP4.5 (blue line) and RCP8.5 (red line) and ensemble spread (coloured area), lower Danube river basin.

The mean temperature of the examined reference and the future sub-periods is shown in Table 7. It may be seen that for the near-term period (2031-2050), there is no significant difference between the two scenarios, however there is an average increase in mean temperature of 1.4-1.6°C according to the two RCPs. For the mid-term period (2051-2070), the average warming trend increases up to 1.9°C for the RCP4.5 and 2.7°C for the RCP8.5. In the long-term period (2071-2090), there is a small further increase up to 2°C for the intermediate scenario (RCP4.5), while for the high-emissions scenario (RCP8.5) the average increase is substantially higher (4°C).

Table 7: Ensemble mean temperature for the reference period and the future sub-periods based on the RCP4.5 and RCP8.5, lower Danube river basin.

Temperature	Reference period	2031-2050		2051-2070		2071-2090	
		RCP4.5	RCP8.5	RCP4.5	RCP8.5	RCP4.5	RCP8.5
Absolute value (°C)	11.3	12.7	12.9	13.2	14	13.3	15.3
Change (°C)		+ 1.4	+ 1.6	+ 1.9	+ 2.7	+ 2	+ 4
Relative change (%)		+ 12	+ 14	+ 17	+ 24	+ 18	+ 35

Regarding the spatial distribution of mean temperature range as this is depicted in Figure 21, there is a great difference between the reference period and the future period based on the two RCPs. The most significant change appears at the area around the Danube river while the change is not so noticeable at the mountainous areas at the northern part of the study area. More specifically, the temperature around the river is between 11 and 13°C during the reference period, while it is projected to be around 13-15°C based on RCP4.5 and is expected to exceed 15°C according to RCP8.5.

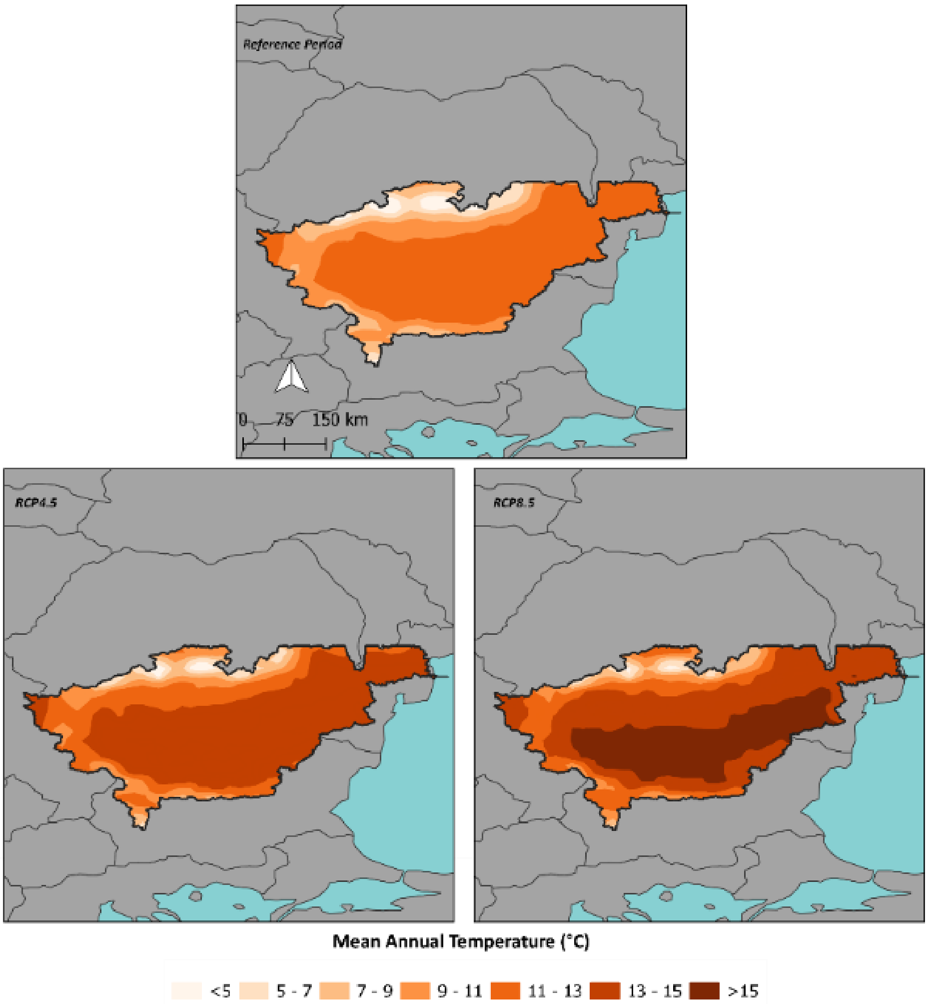

Figure 21: Spatial distribution of the mean annual temperature for the reference period (top) and the future period based on the RCP4.5 and RCP8.5 (bottom), lower Danube river basin.

Precipitation

The projected ensemble mean total precipitation for the two scenarios at the lower Danube river basin, is presented in Figure 22 in the form of annual time series for the period 2031 to 2090. As it may be seen, total precipitation tends to slightly decrease over the 60-year period for both scenarios. The precipitation trends of both scenarios are almost identical during the first decades of the study period while later the precipitation trend of RCP4.5 follows a slightly smaller decrease. Additionally, the average precipitation is above 500mm during the whole period for both RCPs. The minimum precipitation value of the ensemble spread is about 350mm and is observed both at the early years of the period and at the later years. The maximum value of the ensemble spread is observed around 2070 in the case of RCP4.5.

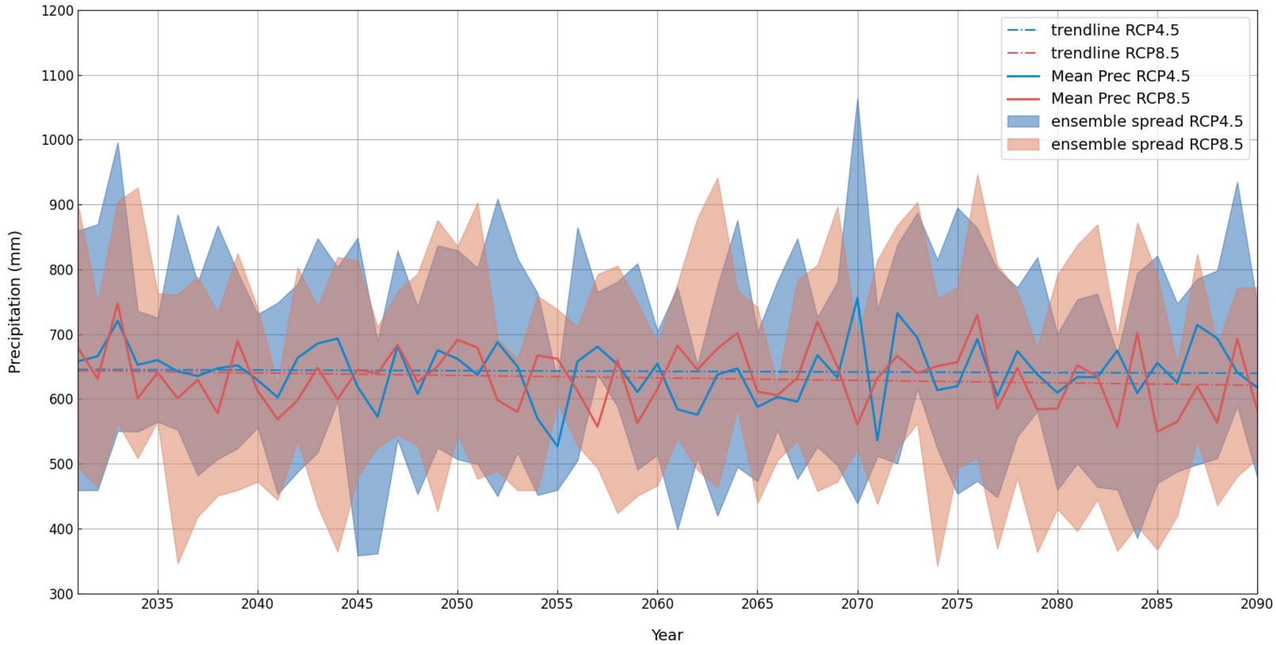

Figure 22: Ensemble mean of total precipitation of the period 2031-2090 for the RCP4.5 (blue line) and RCP8.5 (red line) and ensemble spread (coloured area), lower Danube river basin.

In Table 8, the projected average annual total precipitation for the examined reference and future periods, is provided. It may be concluded that for the near-term period (2031-2050), there is no change in total precipitation for the RCP8.5 while there is an increase of +13mm according to RCP4.5, compared to the reference period. For the mid-term period (2051-2070), the ensemble mean shows slight decreasing trends, about 8mm for the RCP4.5 and 4mm for the RCP8.5, which is not statistically significant reduction, according to Mann-Kendal test. Finally, for the long-term period (2071-2090) there is a small increasing trend about 7mm according to the intermediate scenario, while for the high emissions scenario there is a downward trend of about 13mm.

Table 8: Ensemble mean of total precipitation, for the reference period and the future sub-periods based on the RCP4.5 and RCP8.5, lower Danube river basin.

Precipitation	Reference period	2031-2050		2051-2070		2071-2090	
		RCP4.5	RCP8.5	RCP4.5	RCP8.5	RCP4.5	RCP8.5
Absolute value (mm)	638	651	638	631	634	645	625
Change (mm)		+13	0	-8	-4	+7	-13
Relative change (%)		+2	0	-1	-1	+1	-2

The geospatial distribution of annual precipitation for the different scenarios is depicted in Figure 23. As it may be seen, there is no apparent change between the reference period and the two scenarios, with negligible differences detected, such as in the center of the basin where precipitation is slightly reduced during the future period. Furthermore, maximum values of precipitation above 2000mm are observed at the mountains, while the minimum values below 500mm are observed at the lowlands, according to all scenarios. Finally, the area with the lower precipitation volumes seems to increase for the RCP4.5 compared to reference period, as well as for the RCP8.5 compared to RCP4.5.

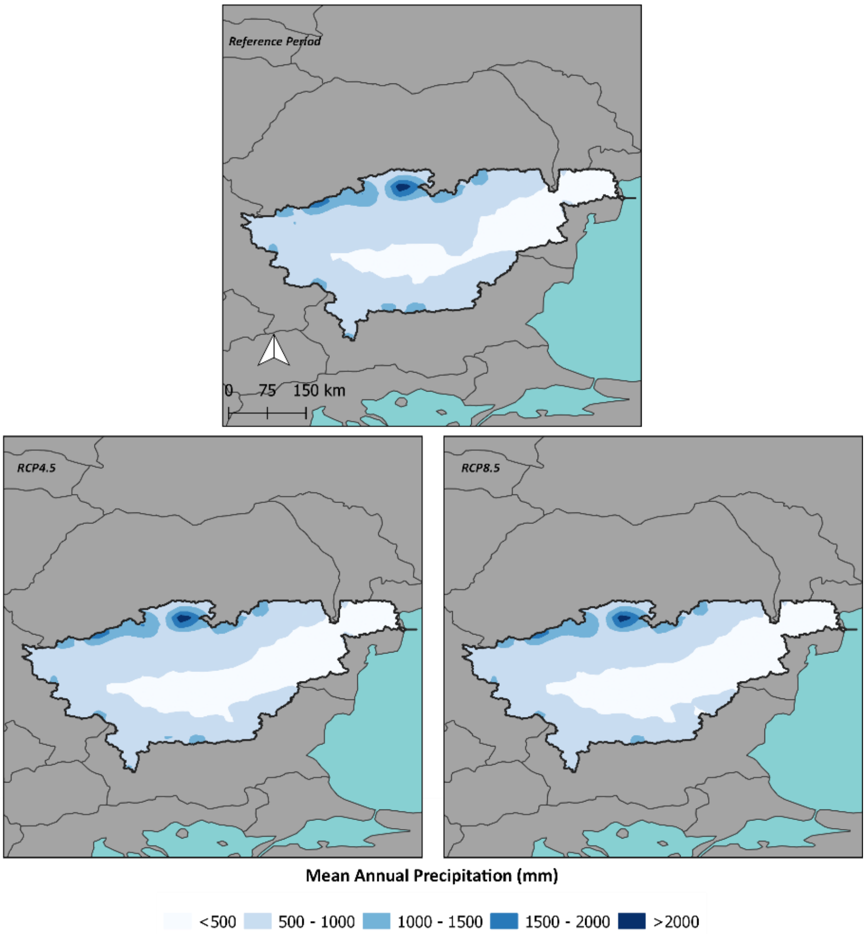

Figure 23: Spatial distribution of the mean annual total precipitation for the reference period (top) and the future period based on the RCP4.5 and RCP8.5 (bottom), lower Danube river basin.

Potential Evapotranspiration

The projected ensemble mean of the mean daily potential evapotranspiration on a monthly basis is presented in Figure 24 in the form of time series for the period 2031-2090, at the lower Danube river basin. As it may be seen, the maximum values are observed during July and the minimum values during December. Both RCPs show increasing trends in daily mean values for all months for the period 2031-2090, in comparison to the reference period. The potential evapotranspiration values for RCP8.5 are higher compared to RCP4.5 which is expected, as the variable follows a very similar pattern to that of temperature. The largest increase in potential evapotranspiration compared to the reference period is observed during May to August, with the month June marking an increase of approximately 17%.

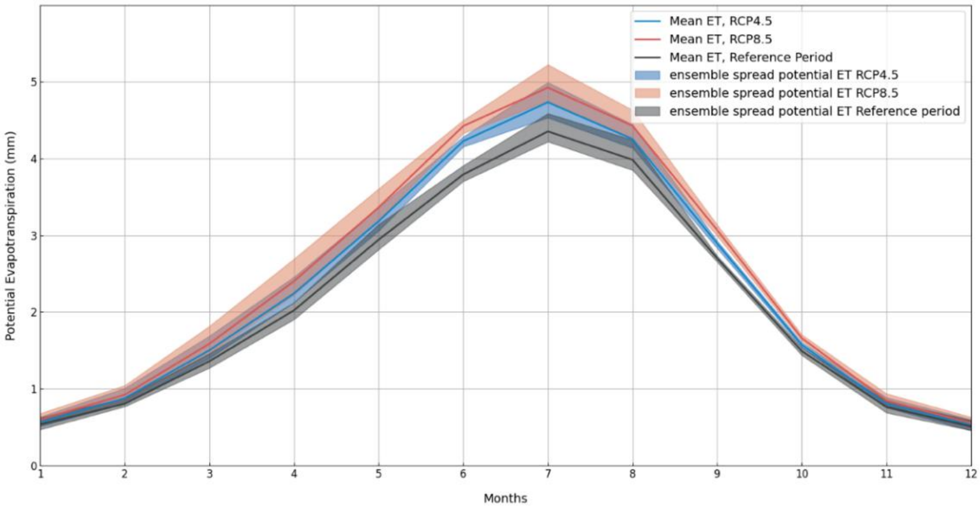

Figure 24: Ensemble mean of the mean daily potential evapotranspiration per month, of the period 2031-2090 for the RCP4.5 (blue line) and RCP8.5 (red line) as well as the reference period 1986-2005 (grey line) and ensemble spread (coloured area), lower Danube river basin.

The spatial distribution of the mean daily potential evapotranspiration range is depicted in Figure 25. It is observed that during the reference period the mean daily potential evapotranspiration range starts from less than 0.5mm at the mountains and up to 3.5mm at the lowlands. The potential evapotranspiration presents increasing trends in the future period (for both scenarios), compared to the reference period. As it is shown, the maximum mean daily potential evapotranspiration increases with a larger part of the area experiencing an increase up to 2.5-3.0mm in potential evapotranspiration. In the case of RCP8.5, an even greater part of the area is expected to experience an increase up to 3.0-3.5mm and even exceed 3.5mm in potential evapotranspiration.

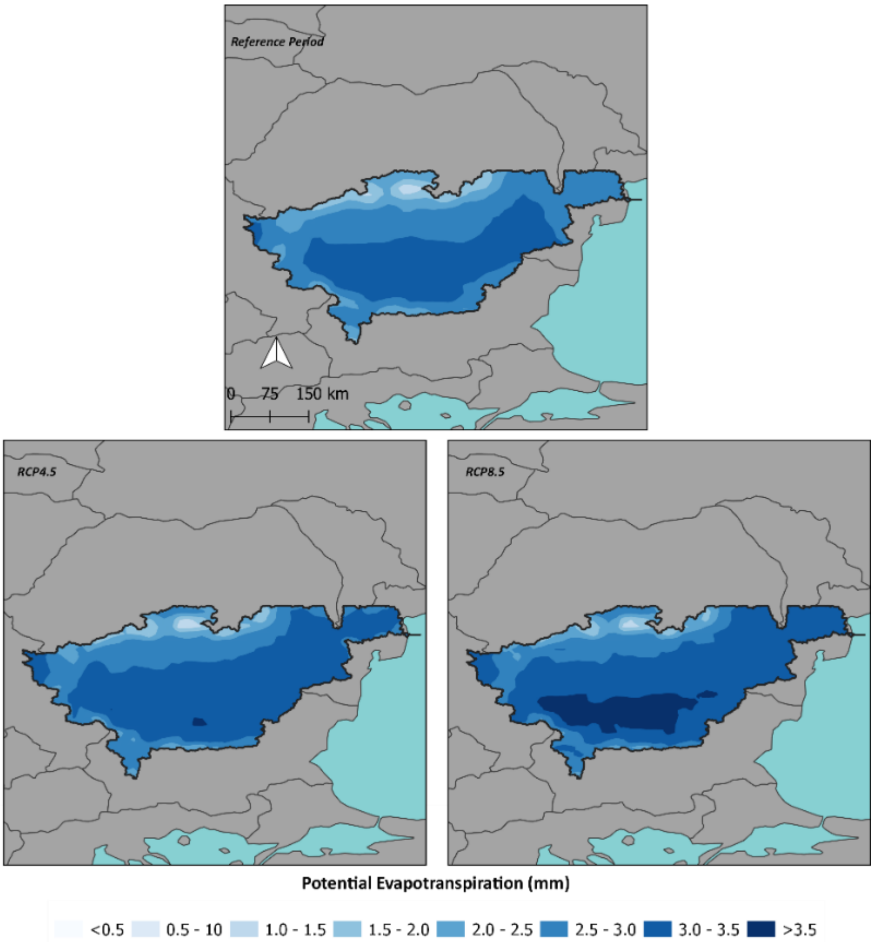

Figure 25: Spatial distribution of the mean daily potential evapotranspiration, for the reference period (top) and the future period based on the RCP4.5 and RCP8.5 (bottom), lower Danube river basin.

3.4 Isonzo-Soča river basin

3.4.1 Pilot area description

The Isonzo, or also known as Soča in Slovenian, is a 140km long river that draws its source in the Julian Alps in Slovenia and joins the Gulf of Trieste at the Northern Adriatic, Italy near Monfalcone, where it forms a delta that tends, over time, to move from west to east. Its catchment area (~3400km^2) consists of mid-altitude mountains (70%), a piedmont (22%), and a coastal plain (8%) influenced by Mediterranean climatic conditions. From the total area of approximately 3400km^2, about 1150km^2, are in Italian territory. The torrent Isonzo-Soča river collects and discharges the waters of the southern side of the Alps Giule, which separate this basin from that of the Sava. It is a fact that, the Italian portion of the Isonzo-Soča river basin coincides for more than 90%, with the sub-basin of the Torre. The mountainous part of the study area is, of low to moderate altitude with mean elevation about 1030 m and the highest point (Triglav) is 2860 m. This area is the interface between two Alpine structural units: (i) the Torre and Natisone basins falling within the Julian Pre-alps (Southern Alps) and (ii) the Isonzo-Soča basin in Slovenia which is part of the Julian Alps. Regarding the climate of the Isonzo-Soča river basin, it has a temperate oceanic climate with influences from the Mediterranean, while at the same time it is presented as zoned. The hydrological regime of the Isonzo-Soča river is determined by precipitation, with a dry season in February and July and two precipitation maxima in fall and spring (Siché & Fassetta, 2014).

In the following maps, the topography and location of the pilot area, as well as, the main land uses/land covers are provided.

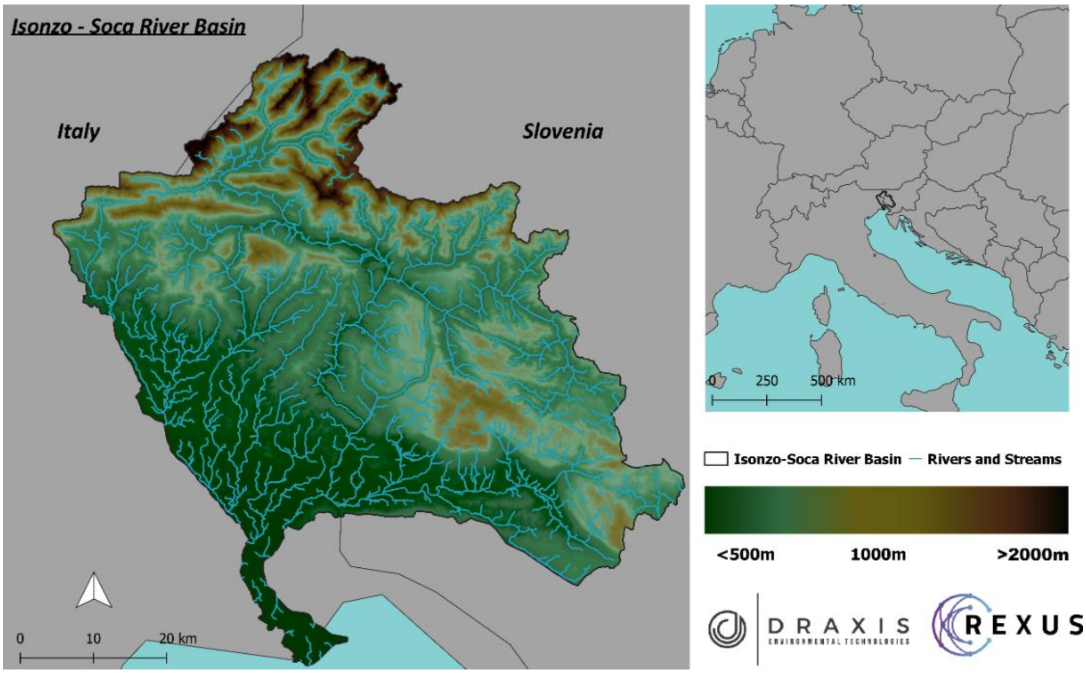

Figure 26: Topographic map of the Isonzo-Soča river basin study area

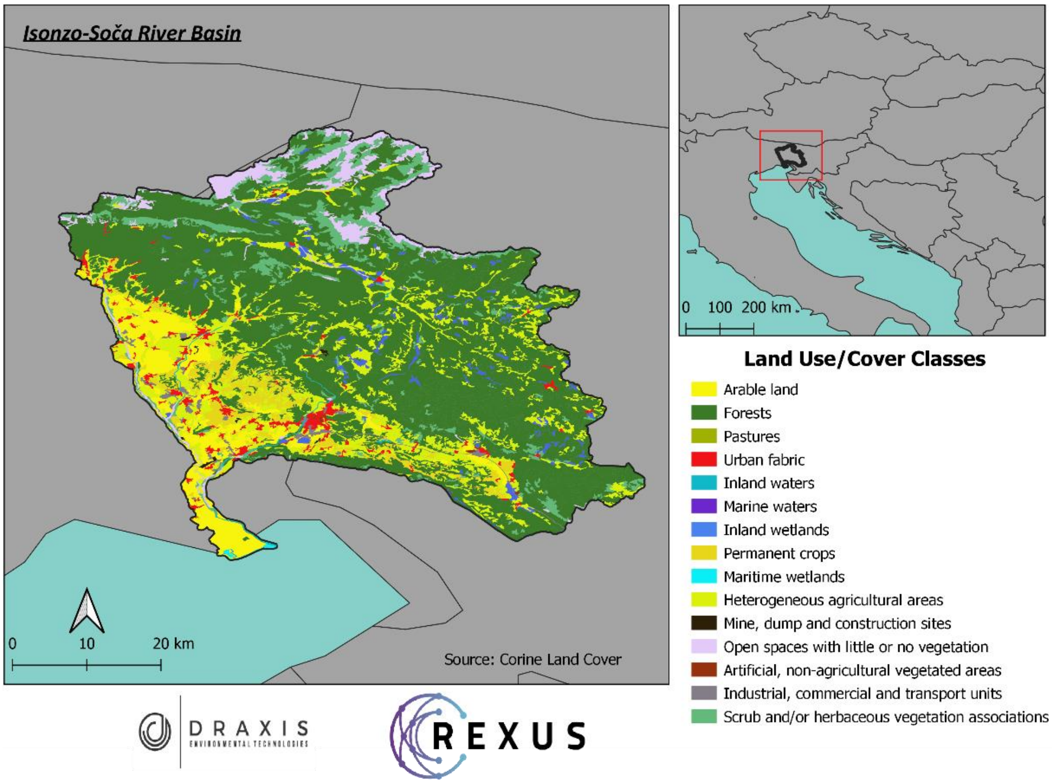

Figure 27: Land use/Land cover map of Isonzo-Soča river basin.

3.4.2 Climate Projections

Temperature

The projected ensemble annual mean temperature for the period 2031-2090, for the pilot of Isonzo-Soča river basin is presented in the form of time series in Figure 28. As it may be observed, there is a clear tendency for temperature increase during the future 60-year period in both scenarios, with the mean temperature staying above 10°C during the whole period. A clear differentiation among the scenarios with more obvious increasing trends for the case of RCP8.5, is observed from 2045 and onwards. The maximum value on the ensemble spread is observed in the case of the RCP8.5 and in specific during the last years of the time series, when it exceeds the value of 17°C. Nevertheless, the ensemble spread for RCP4.5 extends to lower temperatures, especially during the very first years of the study period, when it reaches the minimum mean temperature of almost 6°C.

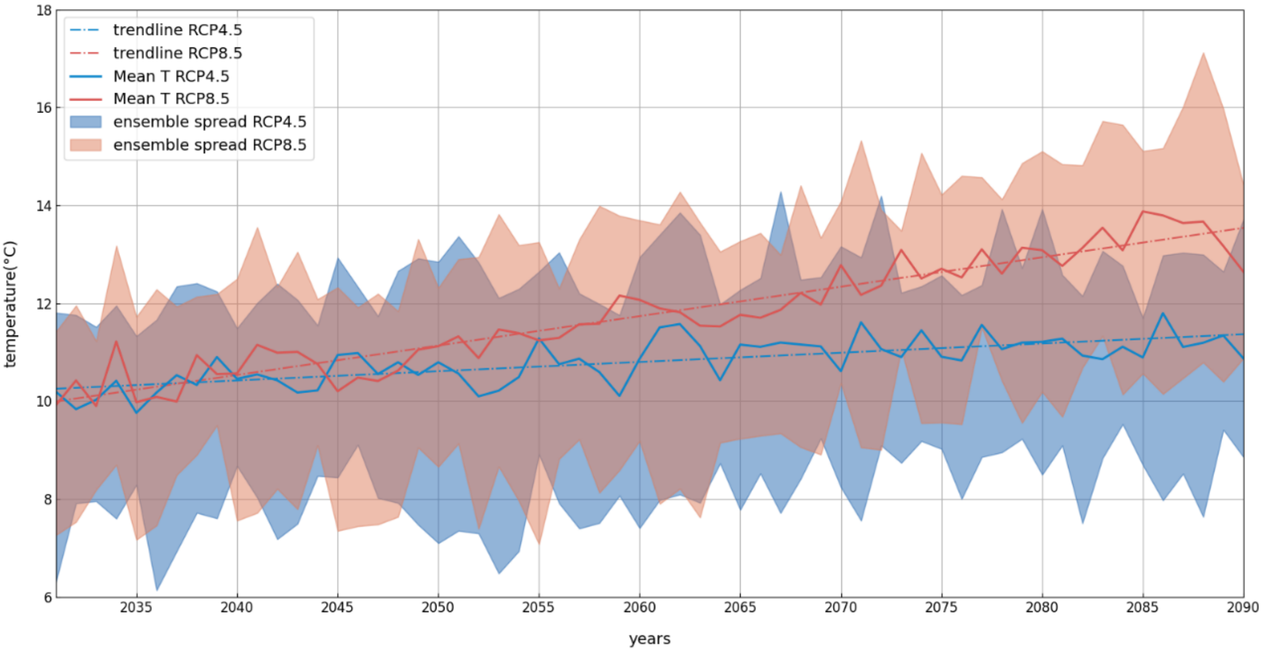

Figure 28: Ensemble mean of mean temperature of the period 2031-2090 for the RCP4.5 (blue line) and RCP8.5 (red line) and ensemble spread (coloured area), Isonzo- Soča river basin.

The mean temperature of the examined reference and future periods is presented in Table 9Table 7. It may be seen that for the near-term period (2031-2050), there is no significant difference between the two scenarios, however there is an average increase in mean temperature of 1.3-1.5°C, compared to the reference period. For the mid-term period (2051-2070), the average warming trend increases up to 1.7°C for the RCP4.5 and 2.6°C for the RCP8.5. In the long-term period (2071-2090), there is a further increase up to 2.1°C for the intermediate scenario (RCP4.5), while for the high-emissions scenario (RCP8.5) the average increase is substantially higher (3.9°C).

Table 9: Ensemble mean temperature for the reference period and the future sub-periods based on the RCP4.5 and RCP8.5, Isonzo- Soča river basin.

Temperature	Reference period	2031-2050		2051-2070		2071-2090	
		RCP4.5	RCP8.5	RCP4.5	RCP8.5	RCP4.5	RCP8.5
Absolute value (°C)	9.1	10.4	10.6	10.8	11.7	11.2	13
Change (°C)		+ 1.3	+ 1.5	+ 1.7	+ 2.6	+ 2.1	+ 3.9
Relative change (%)		+ 14	+ 16	+ 19	+ 29	+ 23	+ 43

Regarding the spatial distribution of mean temperature range as this is depicted in Figure 29, there is a zonal distribution of the values which is decreasing to the northern part of the basin, where the area is more mountainous. It is observed that during the reference period the mean temperature range starts below 4°C at the mountains and reaches up to 12-14°C at the lowlands. During the future period, the maximum mean temperatures are expected to exceed 14°C according to both scenarios, however in the case of RCP8.5, such temperatures are observed at a much greater area. In addition, the respective minimum mean temperatures are increased up to 6°C for the RCP4.5 and up to 8°C for the RCP8.5.

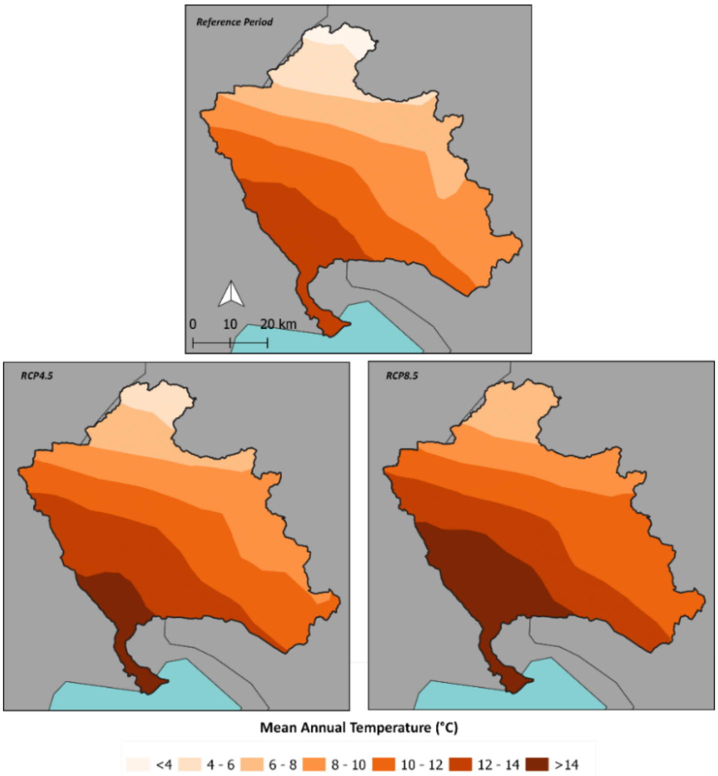

Figure 29: Spatial distribution of the mean annual temperature for the reference period (top) and the future period based on the RCP4.5 and RCP8.5 (bottom), Isonzo-Soča river basin.

Precipitation

The projected ensemble mean total precipitation for the period 2031 to 2090 for the two scenarios at Isonzo-Soča river basin is presented in the form of annual time series in Figure 30. As it may be observed, there is no significant trend in mean annual total precipitation foreseen based on both scenarios, with the average precipitation being above 1400mm during the whole period. The minimum precipitation value of the ensemble spread is about 800mm and is frequently observed within the study period for both scenarios. The maximum value of the ensemble spread is about 2800mm and is observed after 2060 for RCP8.5. It is noteworthy that there are several years after 2060 where the average total precipitation is higher in the case of RCP8.5 than of RCP4.5, however the ensemble spread is wide reflecting the high uncertainty associated to the specific results.

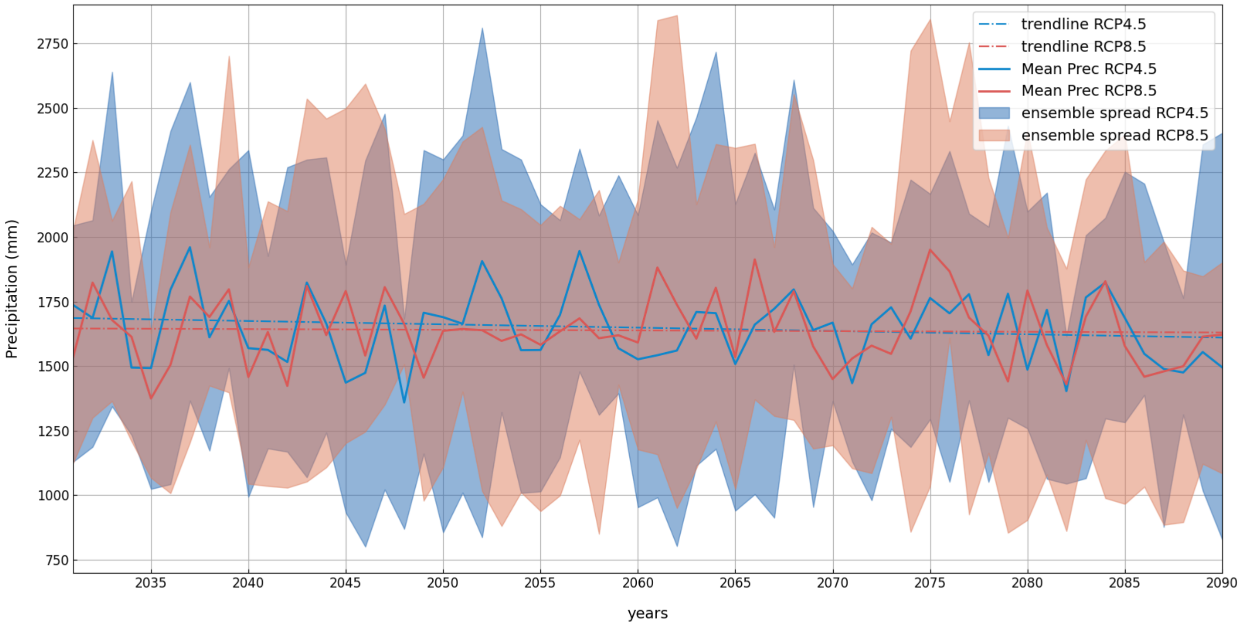

Figure 30: Ensemble mean of total precipitation of the period 2031-2090 for the RCP4.5 (blue line) and RCP8.5 (red line) and ensemble spread (coloured area), Isonzo-Soča river basin.

In Table 10, the projected average annual total precipitation for the examined reference and future sub-periods, is provided. As it may be seen, the average increase in precipitation for the near-term period (2031-2050) is statistically insignificant ranging between 2-3% compared to the reference period. For the mid-term period (2051-2070), the ensemble mean shows slightly higher increasing trends (4-5%), while for the long-term period (2071-2090) the increasing trend decreases again to 2% according to both scenarios.

Table 10: Ensemble mean of total precipitation, for the reference period and the future sub-periods based on the RCP4.5 and RCP8.5, Isonzo-Soča river basin.

Precipitation	Reference period	2031-2050		2051-2070		2071-2090	
		RCP4.5	RCP8.5	RCP4.5	RCP8.5	RCP4.5	RCP8.5
Absolute value (mm)	1597	1650	1631	1672	1657	1622	1625
Change (mm)		+ 53	+ 34	+ 75	+ 60	+ 25	+ 28
Relative change (%)		+ 3	+ 2	+ 5	+ 4	+ 2	+ 2

The geospatial variation of the precipitation for the different scenarios is depicted in Figure 31. As it may be seen, in the reference period 1986-2005, the greatest amount of rain is expected to be experienced at the mountainous parts at the northern part of the basin, as well as at the south-eastern part of the study area, where the altitudes are greater than 1000m. On the other hand, the smallest amounts of rain are observed at the southern part of the basin, where the changes between the reference period and future scenarios are negligible. At the center of the Isonzo-Soča river basin, a small increase in precipitation can be noted for both scenarios. In addition, at higher altitudes there is an insignificant increase in the future period, for RCP4.5, while for RCP8.5 a minor decrease at the same area is observed.

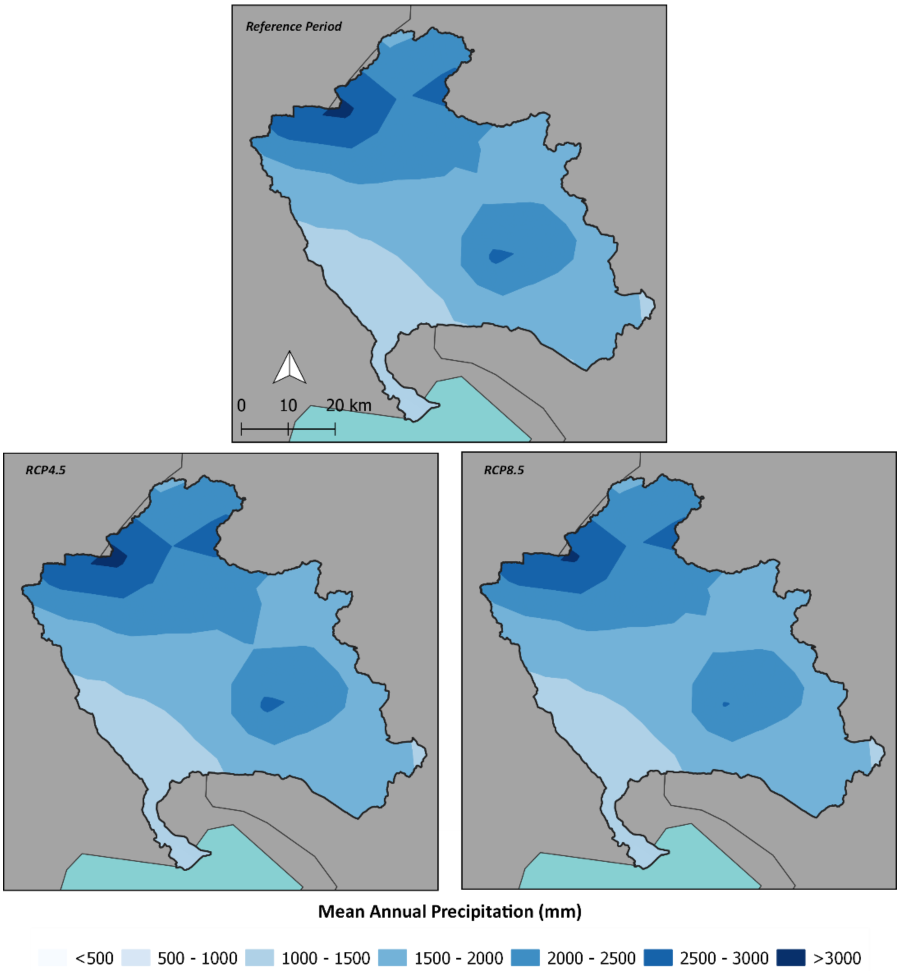

Figure 31: Spatial distribution of the mean annual total precipitation for the reference period (top) and the future period based on the RCP4.5 and RCP8.5 (bottom), Isonzo-Soča river basin.

Potential evapotranspiration

The projected ensemble mean of the mean daily potential evapotranspiration on a monthly basis for the Isonzo-Soča river basin is presented in Figure 32, in the form of time series for the period 2031-2090. Both RCPs show increasing trends in daily mean values for all months for the period 2031-2090, in comparison to the reference period. Comparing the RCP4.5 and RCP8.5, it is observed that the increase in all months is greater for RCP8.5, however, during the colder months (November to February) the changes are negligible. The absolute maximum is observed during July, while the minimum values are observed during December and January. The largest increase in potential evapotranspiration compared to the reference period is observed in July, with approximately 12% relative change.

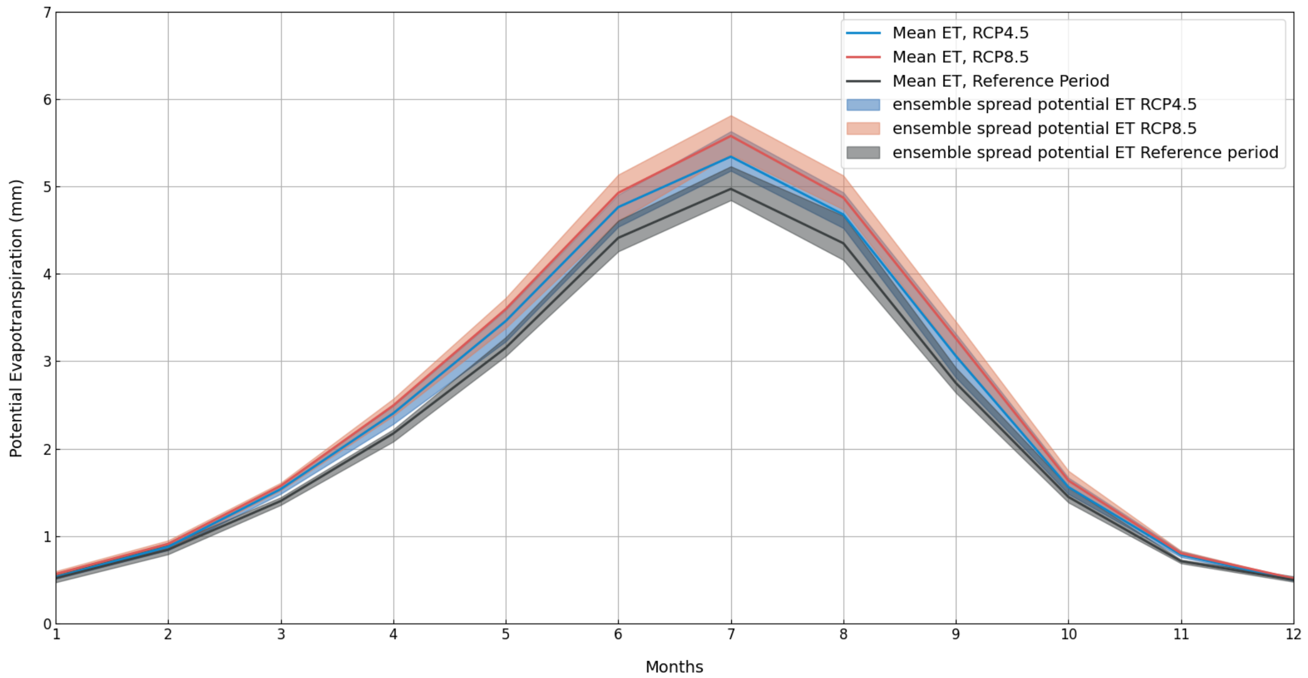

Figure 32: Ensemble mean of the mean daily potential evapotranspiration per month, of the period 2031-2090 for the RCP4.5 (blue line) and RCP8.5 (red line) as well as the reference period 1986-2005 (grey line) and ensemble spread (coloured area), Isonzo-Soča river basin.

The spatial distribution of the mean daily potential evapotranspiration is depicted in Figure 33. It is observed that during the reference period, the mean daily potential evapotranspiration range starts from less than 1.5mm at the north mountainous part and reaches up to 3mm at the southern lowland part. The potential evapotranspiration presents increasing trends during the future period according to both scenarios, in comparison with the reference period. In specific for RCP4.5, the maximum mean daily potential evapotranspiration remains similar to the reference period (2.5-3mm), however this range is observed at a greater area compared to the reference period. For the RCP8.5, the respective values exceed 3mm, at the southern part of the basin.

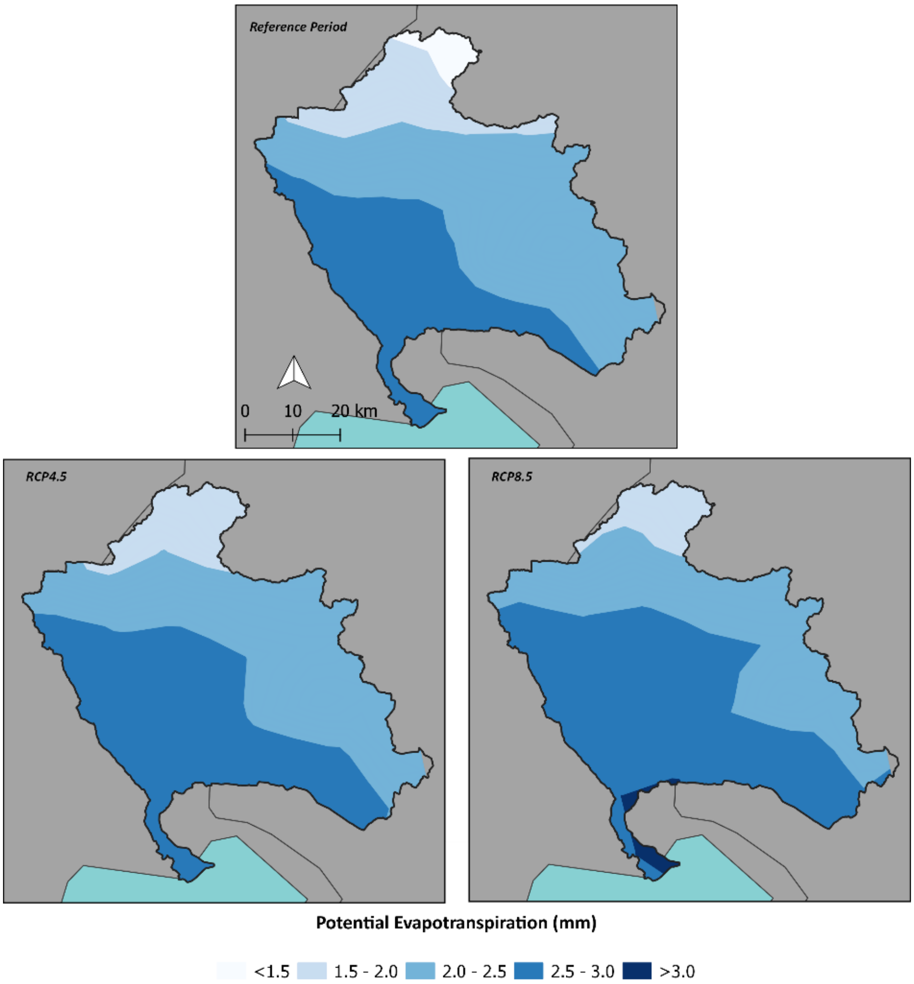

Figure 33: Spatial distribution of the mean daily potential evapotranspiration, for the reference period (top) and the future period based on the RCP4.5 and RCP8.5 (bottom), Isonzo-Soča river basin.

3.5 Nima-Amaime Subwatershed

3.5.1 Pilot area description

The Nima river is a tributary of the Amaime river that drains into the Cauca river, one of the most important rivers of Colombia. The Nima-Amaime subwatershed includes nineteen tributary streams which drain into the Nima river and covers an area of 167km^2, at the southeast of the Department of Cauca Valley. The altitude of the area ranges from 1,050 up to 4,100m at the mountains of the Colombian Andes. The Nima-Amaime subwatershed has a bimodal precipitation regime, with few variations, due to the Pacific equatorial current's convergence of the north-easterly and south-easterly winds. This bimodal pattern is characterised by a rainy season from April to June and September to December, separated by dry seasons in January to March and from June to September (Berrío et al., 2002). The climate of the study area is classified as tropical and has a significant amount of precipitation during the year, even for the driest month. The Köppen-Geiger climate classification for the Nima-Amaime subwatershed is Tropical rainforest climate (Af) (“Climate-data.org”, n.d.).

In the following maps, the topography and location of the pilot area, as well as, the main land uses/land covers are provided.

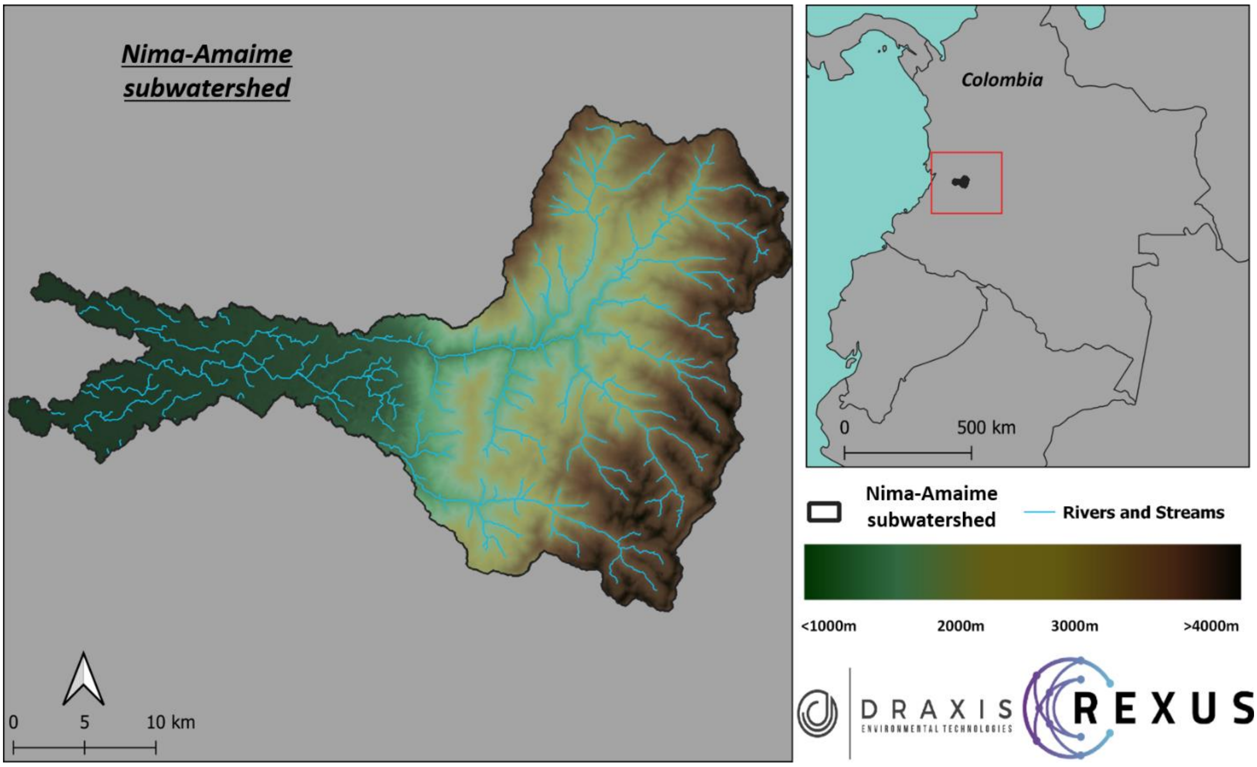

Figure 34: Topographic map of the Nima-Amaime subwatershed study area

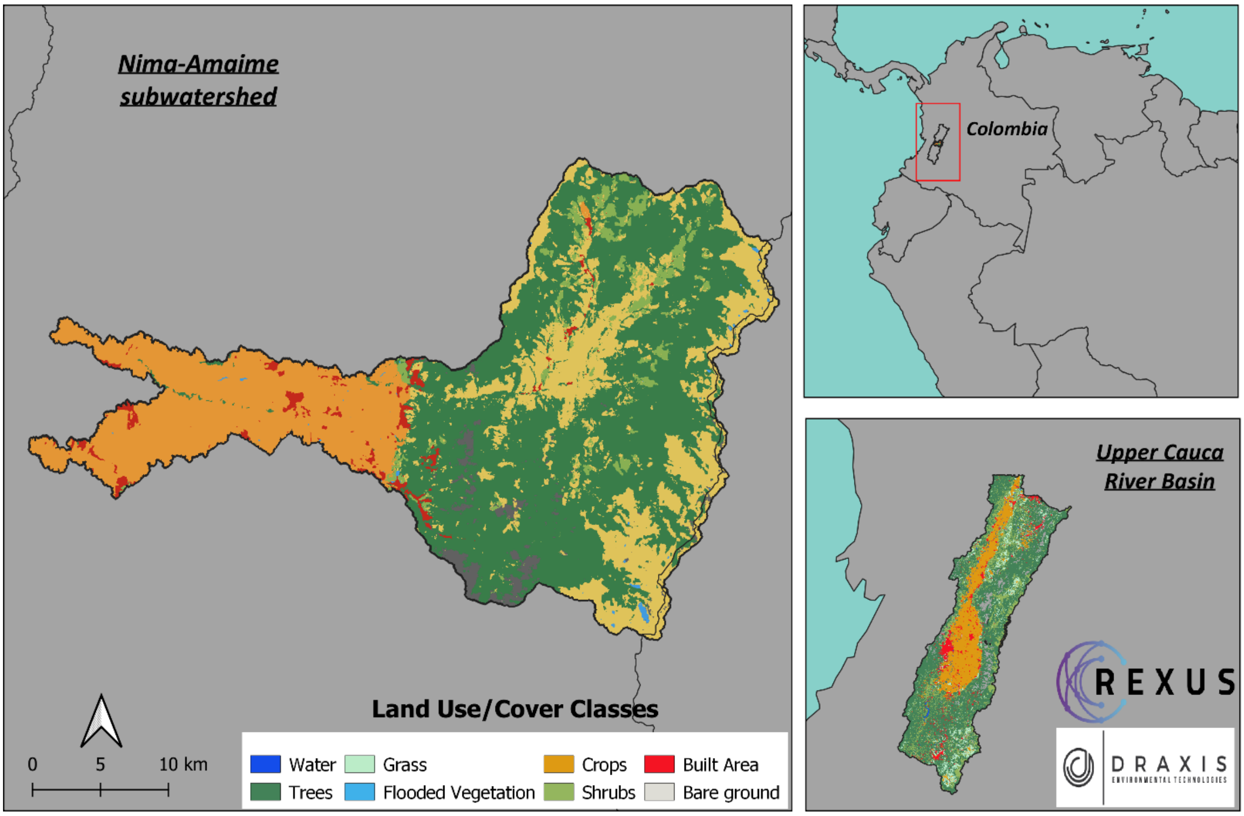

Figure 35: Land use/Land cover map of the Nima-Amaime subwatershed, as well as for the Upper Cauca river basin.

3.5.2 Climate Projections

Temperature

The projected ensemble annual mean temperature for the period 2031-2090, for the pilot of Nima-Amaime subwatershed, is presented in the form of time series in Figure 36. As it may be observed, there is a clear tendency for temperature increase during the future 60-year period in both scenarios, with the mean temperature being above 17°C for the whole period. The RCP8.5 shows a higher increasing trend from the start of the study period, when the ensemble mean temperature is 17-18°C and reaching the highest peak of 21°C in the period 2085-2090. For the same period, the ensemble spread is approximately is ±0.7°C. On the other hand, the ensemble spread for RCP4.5 is wider during the whole period under study, with the widest spread observed during the mid-term period where the ensemble spread is approximately is ±1°C.

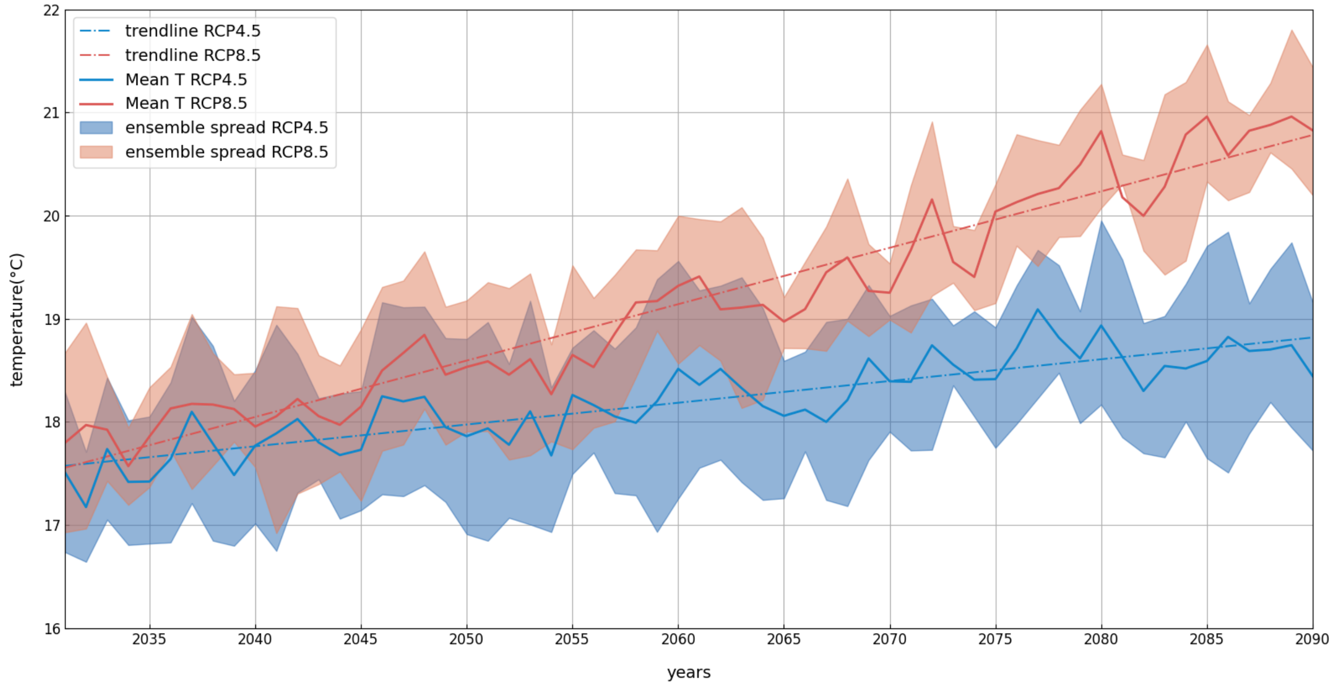

Figure 36: Ensemble mean of mean temperature of the period 2031-2090 for the RCP4.5 (blue line) and RCP8.5 (red line), Nima-Amaime subwatershed.

The mean temperature of the examined reference and future sub-periods is shown in Table 11. It may be seen that for the near-term period (2031-2050) there is no significant difference between the two scenarios while the change compared to the reference period is negligible (up to +0.2°C). In addition, according to RCP4.5 a small average increase is foreseen, reaching the increase of +0.7°C in the long-term period, while according to the RCP8.5, the respective increase in the long-term period is expected to be more pronounced (+2.5°C).

Table 11: Ensemble mean temperature for the reference period and the future sub-periods based on the RCP4.5 and RCP8.5, Nima-Amaime subwatershed.

Temperature	Reference period	2031-2050		2051-2070		2071-2090	
		RCP4.5	RCP8.5	RCP4.5	RCP8.5	RCP4.5	RCP8.5
Absolute value (°C)	17.9	17.9	18.1	18.2	19	18.6	20.4
Change (°C)		0	+ 0.2	+ 0.3	+ 1.1	+ 0.7	+ 2.5
Relative change (%)		0	+ 1	+ 2	+ 6	+ 4	+ 14

The spatial distribution of mean temperature in the Nima-Amaime subwatershed is depicted in Figure 37. Due to lack of high resolution data from the existing climate datasets for the study area, it was considered best to also include the wider Upper Cauca river basin, so as for the reader to have a better overall picture of the climate of the wider area. It is observed that during the reference period the mean temperature range is 10-13°C at the eastern mountainous part of the Nima-Amaime subwatershed and reaches up to 16-19°C at the western lowland part of the study area. During the future period, the maximum mean temperatures increase up to 19-22°C for RCP4.5. In the case of RCP8.5, the mean temperature observed throughout the study area is increased by one temperature class compared to the reference period, as shown in the figure next.

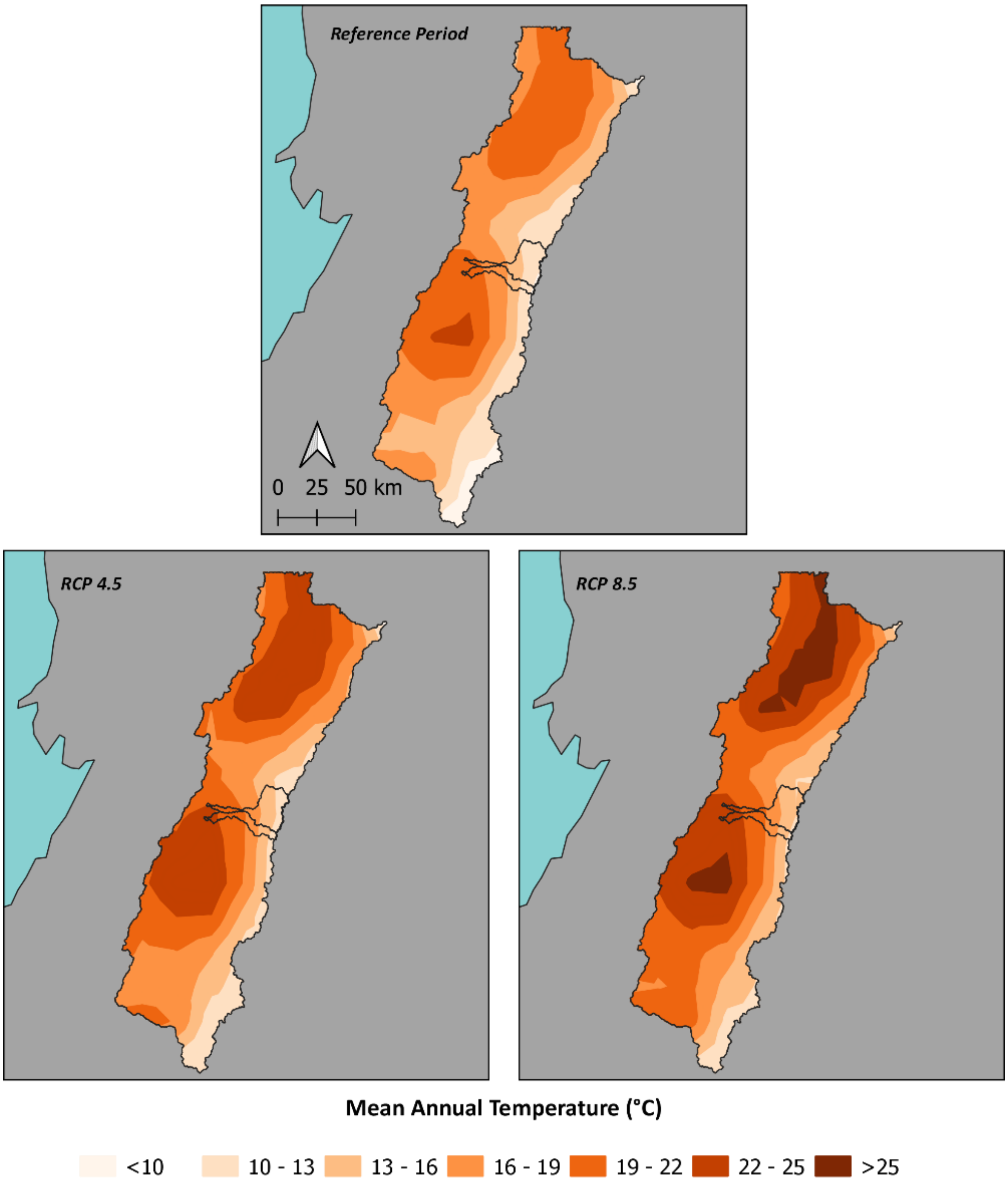

Figure 37: Spatial distribution of the mean annual temperature for the reference period (top) and the future period based on the RCP4.5 and RCP8.5 (bottom), Upper Cauca river basin.

Precipitation

The projected ensemble mean total precipitation for the two scenarios at Nima-Amaime subwatershed, is presented in Figure 38, in the form of annual time series for the period 2031 to 2090. As it may be seen, total precipitation tends to decrease over the 60-year period for both scenarios. Additionally, the mean total precipitation is above 800mm, during the whole period for the RCP4.5 and for the reference period, while for the RCP8.5, precipitation falls below this threshold during the last sub-period 2071-2090. It is worth noting that a peak is observed according to both scenarios, during the period 2045-2050, reaching an average annual precipitation volume of 1500-1600mm. A second noticeable peak is also observed during the period 2075-2080, which is expected to exceed 1400mm according to RCP4.5, while the respective peak is considerably lower for RCP8.5.

Figure 38: Ensemble mean of total precipitation of the period 2031-2090 for the RCP4.5 (blue line) and RCP8.5 (red line), Nima-Amaime subwatershed.

In Table 12, the projected average annual total precipitation for the examined reference and future periods for the Nima-Amaime subwatershed, is provided. It may be concluded that for the near-term period (2031-2050), similar increasing trends are expected for both scenarios (218-232mm or +23-24%) in relation to the reference period. During the mid-term period (2051-2070) the increasing trend is intercepted, as the change observed compared to the reference period is insignificant for both scenarios (+1% for RCP4.5 and -4% for RCP8.5). For the long-term period (2071-2090), the projection trends of the mean total precipitation diverge for the two RCPs, as an average increase of 86mm is foreseen according to RCP4.5, while a substantial average decrease of -284mm is foreseen according to RCP8.5.

Table 12: Ensemble mean of total precipitation, for the reference period and the future sub-periods based on the RCP4.5 and RCP8.5, Nima-Amaime subwatershed.

Precipitation	Reference period	2031-2050		2051-2070		2071-2090	
		RCP4.5	RCP8.5	RCP4.5	RCP8.5	RCP4.5	RCP8.5
Absolute value (mm)	965	1198	1184	975	926	1051	681
Change (mm)		+ 233	+ 219	+ 10	-39	+ 86	-284
Relative change (%)		+ 24	+ 23	+ 1	-4	+ 9	-29

The geospatial variation of the precipitation in the Nima-Amaime subwatershed, including the wider upper Cauca river basin, for the different scenarios is depicted in Figure 39. In the Nima-Amaime subwatershed, the total precipitation is between 1900-2200mm at the eastern part and 1600-1900mm at the western part, for the reference period. For the RCP4.5, the precipitation ranges from 1300 to 1600mm at the major part of the study area, while for the RCP8.5, the precipitation ranges from 1000 to 1300mm at the mountains, while at the lower parts of the basin the values are further reduced to 500-1000mm.

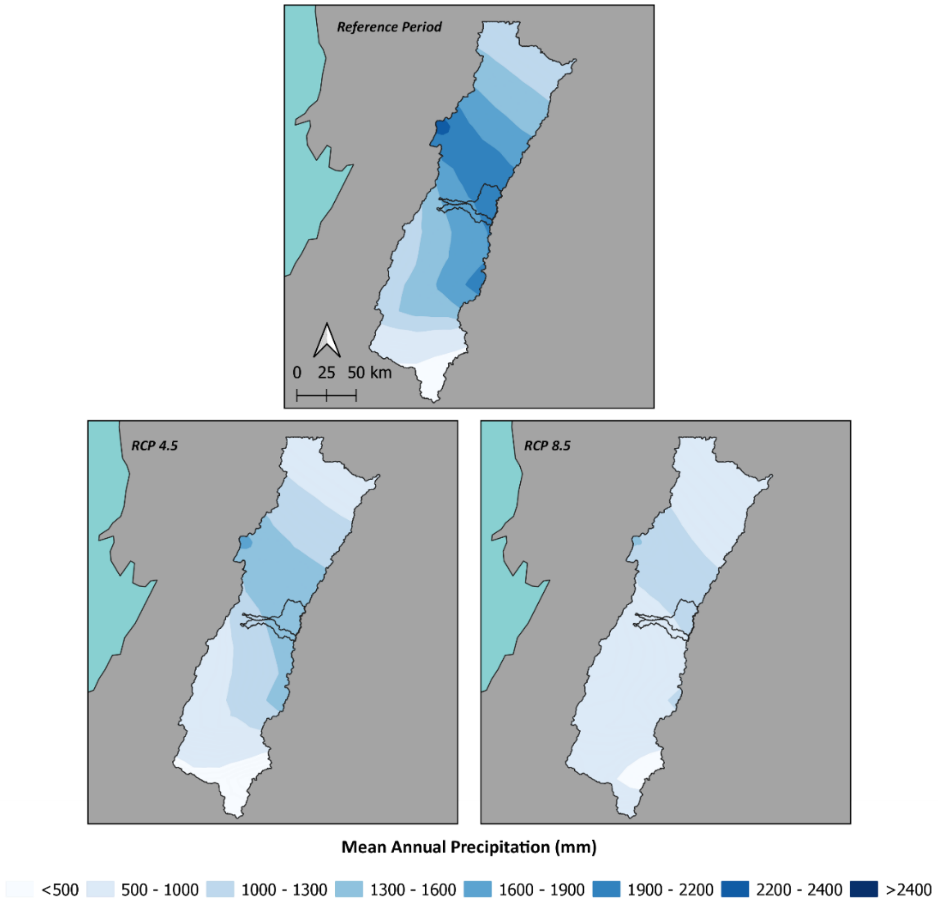

Figure 39: Spatial distribution of the mean annual total precipitation for the reference period (top) and the future period based on the RCP4.5 and RCP8.5 (bottom), Upper Cauca river basin.

Potential Evapotranspiration

The projected ensemble mean of the mean daily potential evapotranspiration on a monthly basis for the Nima-Amaime subwatershed, is presented in Figure 40 in the form of time series for the period 2031-2090. The variation between the months during the reference period is quite smooth and is limited to a small range between about 2.3mm in October-November to 3.9mm in July. The distribution could be characterized as bimodal, since there are two maxima and two minima. Both RCPs show increasing trends in daily mean values for all months for the period 2031-2090, in comparison to the reference period, with the RCP8.5 to foresee higher values compared to RCP4.5. The highest increase is foreseen during the month of October (35%).

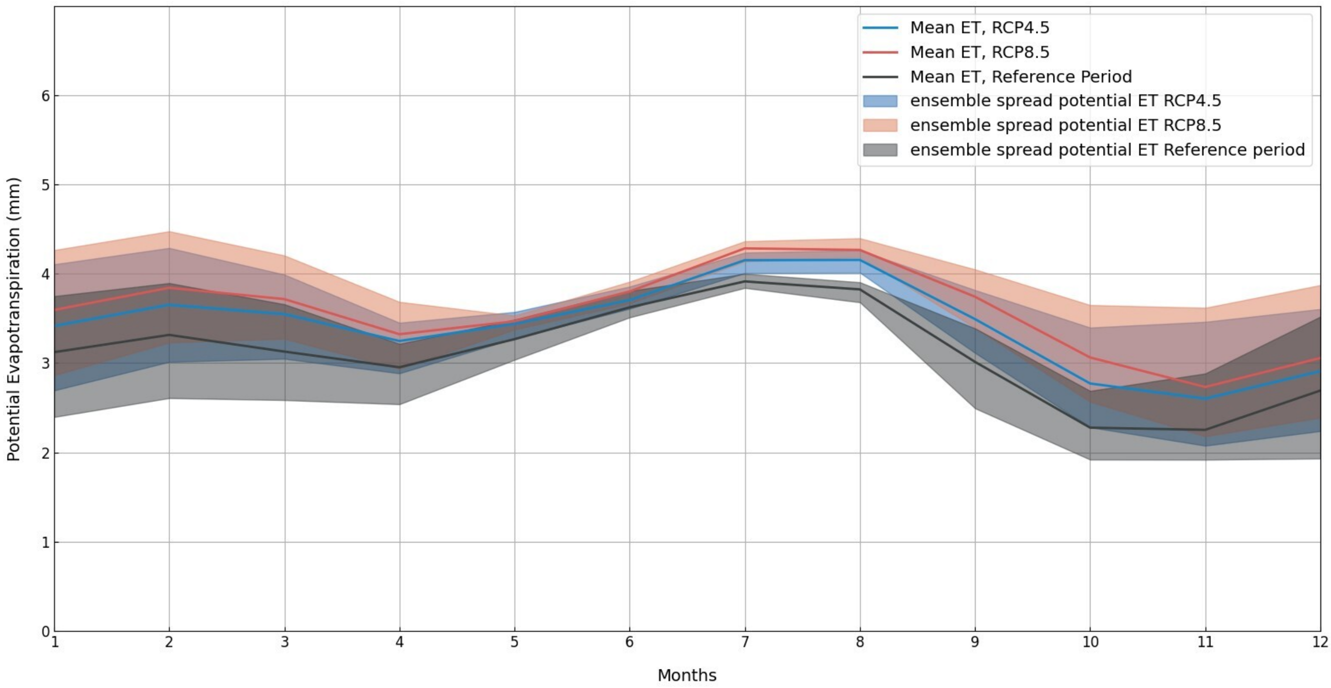

Figure 40: Ensemble mean of the mean daily potential evapotranspiration per month, of the period 2031-2090 for the RCP4.5 (blue line) and RCP8.5 (red line) as well as the reference period 1986-2005 (grey line), Nima-Amaime subwatershed.

The spatial distribution of the mean daily potential evapotranspiration in the Nima-Amaime subwatershed, including the wider upper Cauca river basin, is depicted in Figure 41. It is observed that during the reference period the mean daily potential evapotranspiration range starts from less than 2.4mm at the mountains and up to 3.8mm at the lowlands. During the future period, the maximum mean daily potential evapotranspiration increases and reaches the 4.2mm for RCP4.5, however it is observed only in a limited area. For the RCP8.5, values above 4.4mm are observed in a small area in the northern part of the basin.

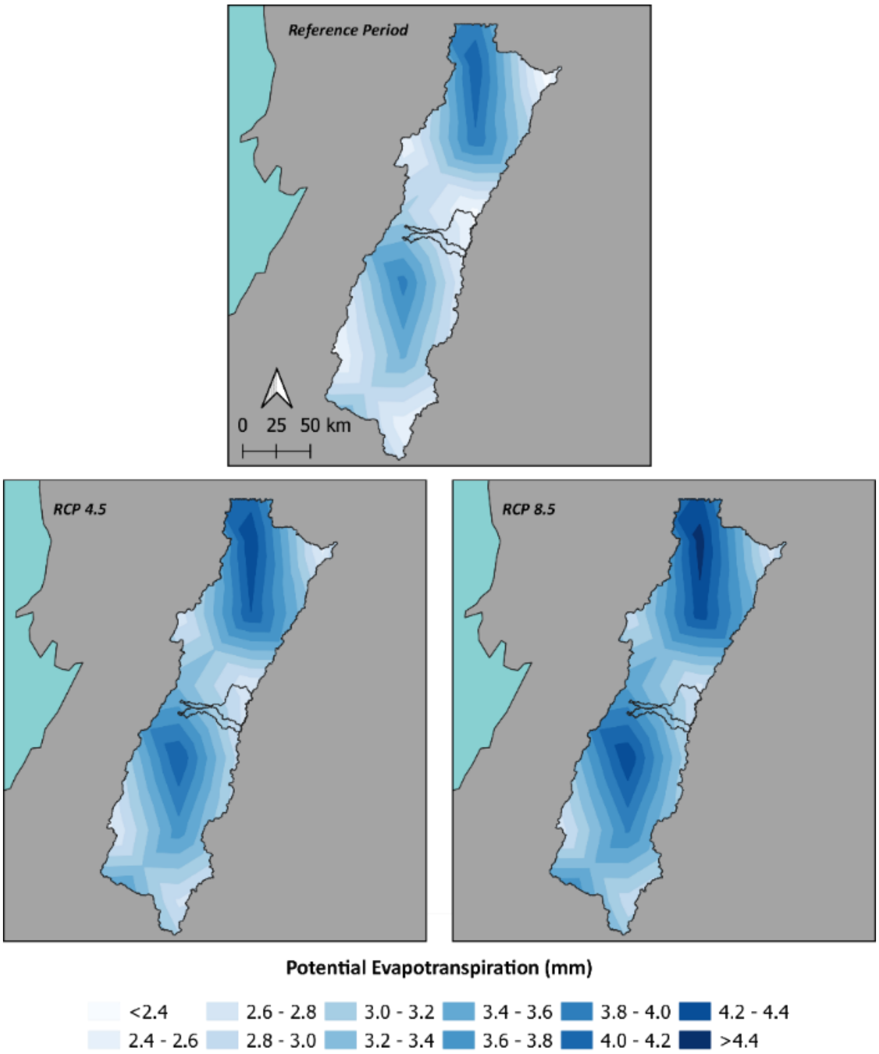

Figure 41: Spatial distribution of the mean daily potential evapotranspiration, for the reference period (top) and the future period based on the RCP4.5 and RCP8.5 (bottom), Nima-Amaime subwatershed.

4 Conclusions

From the analysis of climate projections, it is concluded that, on average, the mean temperature shows a significant increase in the future period (2031-2090) for both scenarios, as well as, for all pilot areas except for the Nima-Amaime subwatershed. According to the results, the average increase in mean temperature on a pilot area basis is expected to be up to +2.1°C based on the RCP4.5, while for the RCP8.5 it may reach up to +4°C. The maximum average increase is observed at the Pinios, the lower Danube and the Isonzo-Soča river basins (3.9-4°C) for the period 2071-2090. In the case of the Nima-Amaime subwatershed, the mean temperature is not expected to change significantly in the short-term. Additionally, the analysis showed that the highest temperature increase is expected to be experienced at the lowlands, whereas the mountainous areas are expected to be less affected.

With respect to precipitation, a decreasing trend is noted for all the pilots according to the two future scenarios, with the exception of the Isonzo-Soča river basin pilot, where the precipitation shows a small increasing trend of up to 5% in the period 2051-2070 based on RCP4.5, however, the ensemble spread of the models' projections is exceptionally wide indicating a higher uncertainty of the results. For the case of Pinios river basin and of the peninsular area of Spain, the average decrease in precipitation reaches up to 12% and 15% respectively, in the 2071-2090 period based on RCP8.5. For the case of the Nima-Amaime subwatershed, the projections show a wide range of precipitation volumes, with an average increase of precipitation up to 24% during the short-term period, while for the long-term period the projections among the scenarios diverge. In specific, an average increase of 9% is foreseen based on RCP4.5, while a substantially higher average decrease of 29% is foreseen based on RCP8.5. Lastly, the precipitation projections for the lower Danube river basin do not show any statistical significant trend. In general, it is observed that the decrease in precipitation is greater at the lowlands and not so intense at the mountains.

The outputs of climate projections for the variable of daily potential evapotranspiration have a similar profile with that of temperature, as increasing trends are observed at all pilot areas and for both future scenarios. The highest average increase in potential evapotranspiration is observed during May-July for all pilots, apart from the case of Nima-Amaime subwatershed, where the highest increase is observed during the months of September-October. of Nima-Amaime subwatershed (~35%) followed by that of the peninsular Spain (~27%), while in the other pilots a lower increase of about 8-12% is expected.

5 References

1. "Climate-data.org". (n.d.). Retrieved from https://en.climate-data.org/south-america/colombia/valle-del-cauca-69/
2. Adopted, IPCC (2014). Climate change 2014 synthesis report. IPCC: Geneva, Szwitzerland. https://ar5-syr.ipcc.ch/ipcc/ipcc/resources/pdf/IPCC_SynthesisReport .pdf
3. Cloke, H. L., Wetterhall, F., He, Y., Freer, J. E., & Pappenberger, F. (2013). Modelling climate impact on floods with ensemble climate projections. Quarterly Journal of the Royal Meteorological Society, 139(671), 282-297. https://doi.org/10.1002/qj.1998.
4. Coordinated Regional Climate Downscaling Experiment. (2021). Retrieved from https://cordex.org/about/
5. Copernicus Climate Change Service (C3S). (2019 August 27). Retrieved from https://cds.climate.copernicus.eu/cdsapp#!/dataset/projections-cordex-domains-single-levels?tab=overview
6. Danforth, Loring, Dimitrov, Philip, Carter, Francis William and Bell, John D. "Bulgaria". Encyclopedia Britannica. (27 September 2021). https://www.britannica.com/place /Bulgaria.
7. Del Rio, Sara & Herrero, L. & Fraile, Roberto & Penas, A. (2011). Spatial distribution of recent precipitation trends in Spain (1961–2006). International Journal of Climatology. 31. 656 - 667. 10.1002/joc.2111.
8. Earth System Grid Federation (ESGF). (2019). Retrieved from https://esgf-data.dkrz.de/search/cordex-dkrz/
9. Fatima, Z., Ahmed, M., Hussain, M., Abbas, G., Ul-Allah, S., Ahmad, S., ... & Hussain, S. (2020). The fingerprints of climate warming on cereal crops phenology and adaptation options. *Scientific reports*, *10*(1), 1-21. https://doi.org/10.1038/s41598-020-74740-3
10. Juan Carlos Berrío, Professor Henry Hooghiemstra, Robert Marchant, Orlando Rangel. (2002). Late-glacial and Holocene history of the dry forest area in the south Colombian Cauca Valley. https://doi.org/10.1002/jqs.701.
11. Katragkou, E., García-Díez, M., Vautard, R., Sobolowski, S., Zanis, P., Alexandri, G., ... & Jacob, D. (2015). Regional climate hindcast simulations within EURO-CORDEX: evaluation of a WRF multi-physics ensemble. Geoscientific model development, 8(3), 603-618. doi:10.5194/gmd-8-603-2015.
12. Kotlarski, S., Keuler, K., Christensen, O. B., Colette, A., Déqué, M., Gobiet, A., ... & Wulfmeyer, V. (2014). Regional climate modeling on European scales: a joint standard evaluation of the EURO-CORDEX RCM ensemble. Geoscientific Model Development, 7(4), 1297-1333. doi:10.5194/gmd-7-1297- 2014.
13. Lemos, M. C., & Rood, R. B. (2010). Climate projections and their impact on policy and practice. Wiley interdisciplinary reviews: climate change, 1(5), 670-682. https://doi.org/10.1002/wcc.71.
14. Liu, K., Harrison, M. T., Archontoulis, S. V., Huth, N., Yang, R., Li Liu, D., ... & Zhou, M. (2021). Climate change shifts forward flowering and reduces crop waterlogging stress. *Environmental Research Letters*, *16*(9), 094017. https://doi.org/10.1088/1748-9326/ac1b5a
15. Mavromatis T., Stathis D., (2011). Response of the Water Balance in Greece to Temperature and Precipitation Trends. Theoretical and Applied Climatology 104:13- 24. doi: 10.1007/s00704-010-0320-9.

16. McSweeney, C. F., Jones, R. G., Lee, R. W., & Rowell, D. P. (2015). Selecting CMIP5 GCMs for downscaling over multiple regions. Climate Dynamics, 44(11), 3237-3260. https://doi.org/10.1007/s00382-014-2418-8
17. Meehl, G.A., T.F. Stocker, W.D. Collins, P. Friedlingstein, A.T. Gaye, J.M. Gregory, A. Kitoh, R. Knutti, J.M. Murphy, A. Noda, S.C.B. Raper, I.G. Watterson, A.J. Weaver and Z.-C. Zhao (2007). Global Climate Projections. In: Climate Change 2007: The Physical Science Basis. Contribution of Working Group I to the Fourth Assessment Report of the Intergovernmental Panel on Climate Change [Solomon, S., D. Qin, M. Manning, Z. Chen, M. Marquis, K.B. Averyt, M. Tignor and H.L. Miller (eds.)]. Cambridge University Press, Cambridge, United Kingdom and New York, NY, USA.
18. Moreno, J. M., Aguiló, E., Alonso, S., Cobelas, M. Á., Anadón, R., & Ballester, F. (2005). A preliminary assessment of the impacts in Spain due to the effects of climate change. *Madrid, SP: Ministerio del Medio Ambiente*.
19. Psomas, A., Dagalaki, V., Panagopoulos, Y., Konsta, D., & Mimikou, M. (2016). Sustainable agricultural water management in Pinios river basin using remote sensing and hydrologic modeling. Procedia engineering, 162, 277-283. https://doi.org/10.1016/j.proeng.2016.11.059
20. Raza, A., Razzaq, A., Mehmood, S. S., Zou, X., Zhang, X., Lv, Y., & Xu, J. (2019). Impact of climate change on crops adaptation and strategies to tackle its outcome: A review. *Plants*, *8*(2), 34. https://doi.org/10.3390/plants8020034
21. Reifen, C., & Toumi, R. (2009). Climate projections: Past performance no guarantee of future skill?. Geophysical Research Letters, 36(13). doi: https://doi.org/10.1029/2009GL038082
22. REXUS project (2021). Baseline description. Deliverable 6.1 – AgriSat. Rexus project HORIZON2020.
23. Robert Mc Sweeney, Zeke Hausfather (2018, January 15). Q&A: How do climate models work?. Carbon Brief. https://www.carbonbrief.org/qa-how-do-climate-models-work
24. Rummukainen, M. (2010). State-of-the-art with regional climate models. Wiley Interdisciplinary Reviews: Climate Change, 1(1), 82-96.doi: https://doi.org/10.1002 /wcc.8
25. Shah, H., Hellegers, P., & Siderius, C. (2021). Climate risk to agriculture: A synthesis to define different types of critical moments. *Climate Risk Management*, 100378. https://doi.org/10.1016/j.crm.2021.100378
26. Siché, I., & Arnaud-fassetta, G. (2014). Anthropogenic actions since the end of the Little Ice Age: A critical factor driving the last 'fluvial metamorphosis' of the Isonzo-Soča river (Italy, Slovenia). Méditerranée: revue géographique des pays méditerranéens, (122), p-183. https://doi.org/10.4000/mediterranee.7253
27. Tabari, H., Marofi, S., Aeini, A., Talaee, P. H., & Mohammadi, K. (2011). Trend analysis of reference evapotranspiration in the western half of Iran. Agricultural and forest meteorology, 151(2), 128-136. https://doi.org/10.1016/j.agrformet.2010.09.009.
28. Tebaldi, C., & Knutti, R. (2007). The use of the multi-model ensemble in probabilistic climate projections. Philosophical transactions of the royal society A: mathematical, physical and engineering sciences, 365(1857), 2053-2075. https://doi.org/10 .1098/rsta.2007.2076.
29. Thomson, Allison & Calvin, Katherine & Smith, Steven & Kyle, Page & Volke, April & Patel, Pralit & Delgado Arias, Sabrina & Bond-Lamberty, Ben & Wise, Marshall & Clarke, Leon & Edmonds, Jae. (2011). RCP4.5: A pathway for stabilization of radiative forcing by 2100. Climatic Change. 109. 77-94. doi: 10.1007/s10584-011-0151-4.

30. Weisheimer, A., Palmer, T. N., & Doblas-Reyes, F. J. (2011). Assessment of representations of model uncertainty in monthly and seasonal forecast ensembles. Geophysical Research Letters, 38(16). https://doi.org/10.1029/2011GL048123.
31. Wilcke, R.A.I. and Bärring, L. (2016). Selecting regional climate scenarios for impact modelling studies. Environmental Modelling & Software 78, 191-201 http://dx.doi.org/10.1016/j.envsoft.2016.01.0
32. WWF factsheet, Green Infrastructure for Europe: The Lower Danube Green Corridor (2015). https://climate-adapt.eea.europa.eu/metadata/case-studies/lower-danube-green-corridor-floodplain-restoration-for-flood-protection/danube_document-1.pdf